frontiers | Frontiers in Plant Science

ORIGINAL RESEARCH
published: 09 September 2022
doi: 10.3389/fpls.2022.962182

Genome-Wide Characterization of Ascorbate Peroxidase Gene Family in Peanut (*Arachis hypogea* L.) Revealed Their Crucial Role in Growth and Multiple Stress Tolerance

Ali Raza[1], Yasir Sharif[2], Kun Chen[2], Lihui Wang[2], Huiwen Fu[2], Yuhui Zhuang[3], Annapurna Chitikineni[4], Hua Chen[1,2], Chong Zhang[1,2], Rajeev K. Varshney[1,4] and Weijian Zhuang[1,2]**

[1] Key Laboratory of Ministry of Education for Genetics, Breeding and Multiple Utilization of Crops, Center of Legume Plant Genetics and Systems Biology, College of Agriculture, Oil Crops Research Institute, Fujian Agriculture and Forestry University (FAFU), Fuzhou, China, [2] College of Plant Protection, Fujian Agriculture and Forestry University (FAFU), Fuzhou, China, [3] College of Life Science, Fujian Agriculture and Forestry University (FAFU), Fuzhou, China, [4] Murdoch's Centre for Crop and Food Innovation, State Agricultural Biotechnology Centre, Food Futures Institute, Murdoch University, Murdoch, WA, Australia

OPEN ACCESS

Edited by:
Shah Fahad,
The University of Haripur, Pakistan

Reviewed by:
Engin Yol,
Akdeniz University, Turkey
Muhammad Azhar Nadeem,
Sivas University of Science and Technology, Turkey

***Correspondence:**
Weijian Zhuang
weijianz@fafu.edu.cn
Rajeev K. Varshney
rajeev.varshney@murdoch.edu.au

Specialty section:
This article was submitted to Plant Abiotic Stress, a section of the journal Frontiers in Plant Science

Received: 06 June 2022
Accepted: 23 June 2022
Published: 09 September 2022

Citation:
Raza A, Sharif Y, Chen K, Wang L, Fu H, Zhuang Y, Chitikineni A, Chen H, Zhang C, Varshney RK and Zhuang W (2022) Genome-Wide Characterization of Ascorbate Peroxidase Gene Family in Peanut (Arachis hypogea L.) Revealed Their Crucial Role in Growth and Multiple Stress Tolerance. Front. Plant Sci. 13:962182. doi: 10.3389/fpls.2022.962182

Ascorbate peroxidase (APX), an important antioxidant enzyme, plays a significant role in ROS scavenging by catalyzing the decrease of hydrogen peroxide under various environmental stresses. Nevertheless, information about the *APX* gene family and their evolutionary and functional attributes in peanut (*Arachis hypogea* L.) was not reported. Therefore, a comprehensive genome-wide study was performed to discover the *APX* genes in cultivated peanut genome. This study identified 166 *AhAPX* genes in the peanut genome, classified into 11 main groups. The gene duplication analysis showed that *AhAPX* genes had experienced segmental duplications and purifying selection pressure. Gene structure and motif investigation indicated that most of the *AhAPX* genes exhibited a comparatively well-preserved exon-intron pattern and motif configuration contained by the identical group. We discovered five phytohormones-, six abiotic stress-, and five growth and development-related *cis*-elements in the promoter regions of *AhAPX*. Fourteen putative ah-miRNAs from 12 families were identified, targeting 33 *AhAPX* genes. Furthermore, we identified 3,257 transcription factors from 38 families (including AP2, ARF, B3, bHLH, bZIP, ERF, MYB, NAC, WRKY, etc.) in 162 *AhAPX* genes. Gene ontology and KEGG enrichment analysis confirm the role of *AhAPX* genes in oxidoreductase activity, catalytic activity, cell junction, cellular response to stimulus and detoxification, biosynthesis of metabolites, and phenylpropanoid metabolism. Based on transcriptome datasets, some genes such as *AhAPX4/7/17/77/82/86/130/133* and *AhAPX160* showed significantly higher

expression in diverse tissues/organs, i.e., flower, leaf, stem, roots, peg, testa, and cotyledon. Likewise, only a few genes, including *AhAPX4/17/19/55/59/82/101/102/137* and *AhAPX140*, were significantly upregulated under abiotic (drought and cold), and phytohormones (ethylene, abscisic acid, paclobutrazol, brassinolide, and salicylic acid) treatments. qRT-PCR-based expression profiling presented the parallel expression trends as generated from transcriptome datasets. Our discoveries gave new visions into the evolution of *APX* genes and provided a base for further functional examinations of the *AhAPX* genes in peanut breeding programs.

Keywords: abiotic stress, antioxidant, drought, genomics, gene ontology, legume, miRNAs, stress responses

INTRODUCTION

Plants are regularly subjected to various environmental factors (abiotic and biotic), which substantially influence crop productivity and cause challenges to food security (Sabagh et al., 2021; Mir et al., 2022; Raza et al., 2022a,b; Saeed et al., 2022; Sharma et al., 2022). These factors can enhance the generation of reactive oxygen species (ROS), damaging cellular systems and supermolecules consisting of DNA, proteins, and lipids, and ultimately leading to cell death (Fahad et al., 2015, 2017; Mittler, 2017; Hasanuzzaman et al., 2020). ROS are mainly produced in different locations including chloroplast, apoplast, plasma membrane, mitochondrion, endoplasmic reticulum, peroxisomes, and cell walls (Mittler, 2017; Hasanuzzaman et al., 2020). In plants, ROS are formed as chemical by-products due to the imperfect decline of oxygen metabolism. Further, ROS are considered as signaling elements that regulate stress tolerance mechanisms in plant molecular biology (Das and Roychoudhury, 2014; Mittler, 2017; Hasanuzzaman et al., 2020). Current progress has revealed that ROS homeostasis is essential for maintaining typical cellular characteristics (Mittler, 2017; Hasanuzzaman et al., 2020, 2021). Subsequently, for regular ROS signaling, plants have developed defense systems including enzymatic and non-enzymatic antioxidant enzymes to maintain the equilibrium between ROS-scavenging and production under stress conditions (Das and Roychoudhury, 2014; Mittler, 2017; Hasanuzzaman et al., 2020, 2021).

In plants, among diverse antioxidant enzymes entailed in ROS-scavenging mechanisms, ascorbate peroxidase (APX; EC, 1.11.1.11) belongs to the heme peroxidase superfamily (Hodges et al., 1999; Teixeira et al., 2004; Lazzarotto et al., 2011). In higher plants, APXs are one of the main antioxidant enzymes involved in regulating the ascorbate-glutathione cycle and take parts to scavenge hydrogen peroxide (H_2O_2) from chloroplast and the cytoplasm. Mainly, it utilized the ascorbic acid as an electron giver to scavenge H_2O_2 generated in plants and thus enhances tolerance to oxidative and other stresses in plants (Cao et al., 2017; Pandey et al., 2017; Hasanuzzaman et al., 2021; Raza et al., 2021a). Additionally, APX enzymes are automated by *APX* gene family involved in stress tolerance has been thoroughly explored in diverse plant species using various *in silico* approaches. For example, five *APX* genes have been discovered in wild watermelon (*Citrullus lanatus*) (Malambane et al., 2018); six in shrub (*Ammopiptanthus nanus*) (Wang et al., 2022); eight in rice (*Oryza sativa* L.) (Teixeira et al., 2004) and *Arabidopsis thaliana* (Panchuk et al., 2002, Panchuk et al., 2005); nine in sorghum (*Sorghum bicolor* L.) (Akbudak et al., 2018); 13 in kiwifruit (*Actinidia chinensis*) (Liao et al., 2020); 16 *APX* genes in tomato (*Solanum lycopersicum* L.) (Najami et al., 2008); 21 in wheat (*Triticum aestivum* L.) (Tyagi et al., 2020); and 26 in cotton (*Gossypium hirsutum* L.) (Tao et al., 2018). Nevertheless, the *APX* gene family in peanut (*Arachis hypogea* L.) has not been systematically reported, and their roles in peanut development and stress tolerance still remain ambiguous.

Cultivated peanut/groundnut (*A. hypogaea* L.), an allotetraploid crop, is one of the most valuable and economic oilseed food crops globally (Agarwal et al., 2018; Bertioli et al., 2019; Chen X. et al., 2019; Zhuang et al., 2019). This crop is being widely cultivated in the tropical and subtropical regions globally; however, several abiotic and biotic factors significantly affect its growth and production, including many important agronomic traits (Agarwal et al., 2018; Gangurde et al., 2020, 2021; Kumar et al., 2020; Pandey et al., 2020; Shasidhar et al., 2020; Sinha et al., 2020; Jadhav et al., 2021; Soni et al., 2021; Aravind et al., 2022; Bomireddy et al., 2022; Liu et al., 2022; Patel et al., 2022). Therefore, it is vital to identify new potential genes associated with multiple stress tolerance and trait improvement in peanut for better protein-rich food supply, particularly in Asian and African countries. In this regard, the recently sequenced peanut genome and recent advances in genomics-assisted breeding make it easier for us to carry out a comprehensive systematic analysis of new gene families (Varshney et al., 2019, 2020, 2021a,b). To our best knowledge, *APX* gene family was yet to be comprehensively characterized in peanut. Thus, the current study performed a genome-wide identification and characterized the *APX* gene family in peanut (*AhAPX*). Several *in silico* analysis, such as characterization, genomic evolution, gene structure, conserved motifs, *cis*-regulatory elements, putative miRNA and transcription factors, functional annotations, etc., were utilized to get insights into the novel roles of *AhAPX* genes. Furthermore, their expression profiling in diverse tissues/organs, under phytohormones and abiotic stress conditions were also performed using transcriptome and qRT-PCR techniques. In short, this report offered evolutionary and functional roles of *AhAPX* genes which could open new windows for further functional studies on the novel roles of *AhAPX* genes in peanut breeding programs under stress conditions.

MATERIALS AND METHODS

Discovery and Physicochemical Features of *APX* Genes

As explained earlier (Li et al., 2021; Raza et al., 2021b; Su et al., 2021), two approaches, i.e., BLASTP and the Hidden Markov Model (HMM), were applied to identify *APX* genes in the peanut (*A. hypogea*) genome. The peanut genome sequence was taken from peanut Genome Resource (PGR) database[1] (Zhuang et al., 2019). In the first approach, the sequences of eight *Arabidopsis thaliana APX* genes were gained from TAIR Arabidopsis genome database[2] (Rhee et al., 2003). Then, these sequences were utilized as a query to perform the BLASTP against peanut genome. In the second approach, HMMER 3.1[3] (Finn et al., 2015) software was employed to seek out the *APX* genes with default controls. Later, the HMM file of the ascorbic acid peroxidase domain (PF00141) was retrieved from the Pfam database[4] (El-Gebali et al., 2019). Lastly, the sequences comprising the PF00141 domain were chosen as putative *APX* genes, and finally, 166 *AhAPX* genes were discovered by uniting the results obtained from both approaches in the peanut genome. Following the same approaches, *APX* genes were also discovered in diploid parents, i.e., *A. duranensis* (90 genes; *AdAPX1-AdAPX90*) and *A. ipaensis* (102 genes; *AiAPX1-AiAPX102*). Their genome sequences were downloaded from PeanutBase database[5] (Dash et al., 2016). The detailed information (including gene name, gene ID, and protein sequences) of all identified *APX* genes is given in **Supplementary Table 1**.

Physicochemical features of *AhAPX* were assessed utilizing the ProtParam tool[6] in the ExPASy server (Gasteiger et al., 2005). Subcellular localization of AhAPX proteins was estimated from CELLO v.2.5[7] (Yu et al., 2006). Exon-intron configuration of all *AhAPX* were determined using TBtools software (v1.09867)[8] (Chen et al., 2020). The conserved motifs of AhAPX sequences were documented using the MEME website[9] (Bailey et al., 2009).

Evaluation of Chromosomal Location, Phylogenetic Relationships, and Synteny Analysis of *APX* Genes

The data about the chromosomal location of *AhAPX* was attained from the PGR database, and the TBTools was utilized to map the genes on chromosomes. To discover the evolutionary link of the APX proteins, a phylogenetic tree among *A. hypogea* (AhAPXs), *A. duranensis* (AdAPXs), *A. ipaensis* (AiAPXs), and *A. thaliana* (AtAPXs) was created. Multiple sequence alignment was implemented using MEGA7 software[10] (Kumar et al., 2018). The neighbor-joining (NJ) method was undertaken to design a phylogenetic tree with 1,000 bootstrap replicates and iTOL was used to beautify the tree[11] (Letunic and Bork, 2021).

The syntenic associations of *APX* genes between *A. hypogea*, *A. duranensis*, *A. ipaensis*, and *A. thaliana* were executed through the MCScanX toolkit and were pictured by the Advance Circos package in the TBTools software (Chen et al., 2020). Additionally, the multiple collinearity analysis of *APX* genes was completed *via* multiple synteny Plot packages in TBTools software. The Ka/Ks ratios of all *AhAPX* were predicted *via* simple Ka/Ks calculator in TBTools software.

Prediction of *cis*-Regulatory Elements in the *AhAPX* Promoters

To predict the putative *cis*-regulatory elements in the *AhAPX* promoters, the 2 Kb sequences upstream of start codons were separated from the peanut genome. The promoter sequences of all *AhAPX* genes were observed with PlantCARE website[12] (Lescot et al., 2002), and the picture was illustrated using TBtools software.

Prediction of Putative miRNAs Targeting *AhAPX* Genes and Functional Annotation Evaluation

The CDS of all *AhAPX* was used to predict the miRNA target sites with psRNATarget website[13] (Dai et al., 2018) with default considerations. The interactive network figure among the putative miRNAs and *AhAPX* genes was made *via* Cytoscape software (v3.9)[14] (Shannon et al., 2003). Gene ontology (GO) and Kyoto encyclopedia of genes and genomics (KEGG) annotation evaluation was undertaken by submitting all AhAPX protein sequences to the eggNOG v4.0[15] (Powell et al., 2014). At the same time, GO and KEGG enrichment evaluations were performed with TBtools software.

Prediction of Transcription Factor Regulatory Network of *AhAPX* Genes

To predict the putative transcription factors (TFs) and regulatory network, the 500 bp nucleotide sequences from upstream regions of *AhAPX* genes were removed and complied to the PlantRegMap (Transcriptional Regulatory Map)[16] with p-value $\leq 1e^{-6}$ (Tian et al., 2020). The regulatory network of predicted TFs and *AhAPX* genes was created with Cytoscape v3.9 software.

Expression Profiling of *AhAPX* Genes

The expression levels of all *AhAPX* genes at diverse developmental tissues/organs (embryo, cotyledon, testa, pericarp, peg, root and stem, root nodule, root tip, root, step tip, stem, leaf, and flower), under various hormones (ethylene, abscisic

[1] http://peanutgr.fafu.edu.cn/
[2] http://www.arabidopsis.org/
[3] http://www.hmmer.org/
[4] http://pfam.xfam.org/
[5] https://www.peanutbase.org/
[6] http://web.expasy.org/protparam/
[7] http://cello.life.nctu.edu.tw/
[8] https://github.com/CJ-Chen/TBtools
[9] https://meme-suite.org/meme/db/motifs
[10] https://megasoftware.net/home
[11] https://itol.embl.de/
[12] http://bioinformatics.psb.ugent.be/webtools/plantcare/html/
[13] https://www.zhaolab.org/psRNATarget/home
[14] https://cytoscape.org/download.html
[15] http://eggnog-mapper.embl.de/
[16] http://plantregmap.gao-lab.org/binding_site_prediction.php

acid, paclobutrazol, brassinolide, and salicylic acid), and abiotic stress (drought and cold) conditions were evaluated using openly available transcriptome dataset of cultivated peanut (cultivar Shitouqi) at PGR database (see text footnote 1; BioProject PRJNA480120) (Zhuang et al., 2019). The detailed procedure for sample harvesting and data analysis is presented in our recent paper (Zhuang et al., 2019). Owing to the great differences in the expression trends, we normalize the log2 of fragments per kilobase of transcript per million (FPKM) values. Finally, the circular heat maps were designed by TBtools software.

Plant Material and Stress Conditions

In this study, a widely cultivated peanut variety in southeast China, "Minhua-6" was used for stress treatments. The same variety was also used for transcriptome analysis in our recent paper (Zhuang et al., 2019). The seeds of the "Minhua-6" cultivar were obtained from the FAFU, Fuzhou, China. The vigor seeds were cultured on small pots having a mix of vermicompost. For stress treatment, germinated seedlings at the four-leaf stage were exposed to cold stress at 4°C and ABA (10 $\mu g\ mL^{-1}$) for 0 (CK), 3, 6, 9, and 12 h with three biological repetitions. All of the samples were instantly frozen in liquid nitrogen and were kept at -80°C until RNA extraction.

RNA Extraction and qRT-PCR-based Expression Analysis

Total RNA was isolated utilizing the CTAB method as described in our recent work (Sharif et al., 2021), and cDNA was prepared with the help of Evo M-MLV RT Kit with gDNA Clean for qPCR II (Code No. AG11711; Hunan Aikerui Biological Engineering Co., Ltd., China) following the developer guidelines. The comprehensive information on qRT-PCR reaction has been described in our recent work (Sharif et al., 2021). The peanut *Actin* gene was used as a housekeeping gene to stabilize the expression (Chi et al., 2012). The expression data of three biological repeats were normalized using the $2^{-\Delta\Delta CT}$ method (Livak and Schmittgen, 2001). All the primers used for qRT-PCR are given in **Supplementary Table 2**. The graphs were made with GraphPad Prism v9.0.0 software[17] (Swift, 1997).

RESULTS

Comprehensive Characterization of *AhAPX* Genes in Peanut Genome

In this study, a total of 166 *AhAPX* genes were discovered in the peanut genome (**Table 1**). Henceforward, these genes are labeled as "*AhAPX1–AhAPX166*." These genes were irregularly mapped in the cultivated peanut genome. The maximum number (15) of *AhAPX* genes were mapped on Chr14, followed by Chr04/Chr11 with 11 genes on each chromosome. While, Chr01/Chr06/Chr10/Chr20 were found to have ten genes, followed by Chr05/Chr15/Chr16 with nine genes, Chr07/Chr19 with eight genes, Chr09/Chr13 with seven genes, Chr03/Chr08/Chr17/Chr18 with six genes on each chromosome. The lowest number (1 and 4) of *AhAPX* genes were mapped on Chr02 and Chr12, respectively. Notably, three *AhAPX* genes (*AhAPX1/2/3*) were also mapped on an unassembled region (Chr00) (**Figure 1**).

Comprehensive information of all predicted 166 *AhAPX* genes is presented in **Table 1**. In short, the CDS length varied from 327 bp (*AhAPX71*) to 1,923 bp (*AhAPX25/45*), and the amino acid length assorted from 108 (*AhAPX71*) to 640 (*AhAPX25/45*) amino acids. The number of exons varied from one (*AhAPX43/50/61/117/131/134*) to 16 (*AhAPX45/145*) (**Table 1**). Particularly, only two genes (*AhAPX45* and *AhAPX145*) had the uppermost number of introns (i.e., 15), and quite a few genes lack introns (i.e., *AhAPX43/50/61/117/131/134*) (**Table 1**). The anticipated molecular weights (MW) of the 166 AhAPX proteins increased from 3.85 kDa (AhAPX79) to 70.66 kDa (AhAPX45), the isoelectric points (PI) extended from 4.41 (AhAPX83) to 9.76 (AhAPX51), and the GRAVY ranged from -0.639 (AhAPX145) to 0.392 (AhAPX161). The transformations in MW and PI are primarily due to the elevated content of necessary amino acids and post-translational alterations. The *in silico* subcellular localization discovered that 115 AhAPX proteins were situated on the extracellular matrix, 14 AhAPX proteins on plasma membrane, 12 AhAPX proteins on cytoplasm, nine AhAPX proteins on chloroplast, and five AhAPX proteins on mitochondrion (**Table 1**). Notably, some AhAPX proteins were found to be located in more than one location (**Table 1**).

On the other hand, eight genes (*AtAPXs*) from *A. thaliana*, 90 genes (*AdAPX1-AdAPX90*) from *A. duranensis*, and 102 genes (*AiAPX1-AiAPX102*) from *A. ipaensis* genomes were also recognized to study the evolution of *APX* genes between tetraploid and diploid parents (**Supplementary Table 1**).

Insights From Phylogenetic Relationships of *APX* Proteins

To determine the in-depth evolutionary and phylogenetic history between the AhAPX (166 members), AdAPX (90 members), AiAPX (102 members), and AtAPX proteins (8 members), an unrooted phylogenetic tree was built by a multiple sequence alignment, which was divided into 11 main groups (group1–group11) (**Figure 2**). The discoveries exposed that group1 comprised of seven APX members (2 AhAPX, 2 AiAPX, and 3 AdAPX) followed by group4/5 (eight APX members), and group3 (14 APX members). Notably, the maximum number of APX members (66 AhAPX, 39 AiAPX, and 33 AdAPX) were found in group 11 followed by group7 (38 APX members), group2/6 (37 APX members), group8/9 (28 APX members), and group10 (24 APX members) (**Figure 2**). All AtAPX members were clustered only in one group, i.e., group 2. In general, APXs grouped into the indistinguishable sub-group may retain corresponding functions. It is worth stating that *A. hypogea* APX (AhAPXs) were distributed in each group with homologs from *A. duranensis, A. ipaensis,* and *A. thaliana*., and group11 was detected to have more AhAPX members than the other 10 groups (**Figure 2**). Furthermore, it was observed that the AhAPXs

[17] https://www.graphpad.com/

TABLE 1 | The data of 166 *AhAPX* genes identified in peanut genome.

Gene name	Gene ID	Genomic region	CDS length (bp)	Exon	Intron	Protein length (aa)	MW (KDa)	PI	GRAVY	Subcellular localization
AhAPX1	AH00G01650.1	Chr00 (2097889, 2103344, +)	1260	11	10	419	44.68	8.64	−0.156	Chloroplast
AhAPX2	AH00G03280.1	Chr00 (4356387, 4358168, +)	756	7	6	251	27.79	5.39	−0.491	Cytoplasmic
AhAPX3	AH00G04650.1	Chr00 (6939173, 6940468, −)	987	4	3	328	35.75	6.17	−0.223	Extracellular and nuclear
AhAPX4	AH01G28620.1	Chr01 (102500998, 102502258, −)	1011	4	3	336	37.9	8.48	−0.37	Nuclear
AhAPX5	AH01G31200.1	Chr01 (105607976, 105610045, +)	972	4	3	323	35.1	6.59	−0.101	Extracellular
AhAPX6	AH01G01000.1	Chr01 (1376119, 1378806, −)	1005	4	3	334	36.6	8.23	−0.169	Extracellular
AhAPX7	AH01G11780.1	Chr01 (19611835, 19615124, +)	981	4	3	326	35.23	8.87	−0.056	Extracellular
AhAPX8	AH01G05760.1	Chr01 (7328535, 7331547, +)	969	4	3	322	34.26	6.28	0.029	Extracellular and plasma membrane
AhAPX9	AH01G05770.1	Chr01 (7337595, 7340770, −)	987	3	2	328	36.11	9.57	−0.173	Extracellular
AhAPX10	AH01G05780.1	Chr01 (7349081, 7354713, −)	969	3	2	322	35.44	8.68	−0.441	Nuclear
AhAPX11	AH01G21450.1	Chr01 (93462135, 93464576, +)	987	4	3	328	35.34	6.08	0.017	Extracellular
AhAPX12	AH01G22400.1	Chr01 (94528243, 94529833, +)	990	3	2	329	36.09	9.2	−0.206	Extracellular
AhAPX13	AH01G26210.1	Chr01 (99439266, 99440500, −)	999	4	3	332	35.7	4.5	−0.139	Extracellular
AhAPX14	AH02G25000.1	Chr02 (95622557, 95623515, +)	660	3	2	219	24.43	8.99	−0.35	Extracellular
AhAPX15	AH03G45630.1	Chr03 (139181976, 139183516, +)	966	3	2	321	34	6.51	−0.088	Extracellular
AhAPX16	AH03G12620.1	Chr03 (14627327, 14629723, +)	978	4	3	325	35.45	6.55	−0.021	Plasma membrane
AhAPX17	AH03G01960.1	Chr03 (2186290, 2188245, −)	756	9	8	251	27	5.52	−0.319	Cytoplasmic
AhAPX18	AH03G05320.1	Chr03 (5424432, 5426098, +)	978	4	3	325	34.52	8.71	0.015	Extracellular
AhAPX19	AH03G06180.1	Chr03 (6345566, 6348916, −)	867	9	8	288	31.66	6.67	−0.311	Cytoplasmic
AhAPX20	AH03G07350.1	Chr03 (7481431, 7483098, −)	978	4	3	325	34.61	8.71	0.019	Extracellular and plasma membrane
AhAPX21	AH04G21680.1	Chr04 (106761278, 106763236, +)	954	4	3	317	33.53	8.05	−0.061	Extracellular
AhAPX22	AH04G21700.1	Chr04 (106776477, 106779460, +)	957	4	3	318	34	4.94	−0.057	Extracellular
AhAPX23	AH04G09710.1	Chr04 (16167517, 16170131, +)	912	4	3	303	33.45	7.53	0.003	Extracellular
AhAPX24	AH04G09790.1	Chr04 (16461353, 16464502, −)	1068	4	3	355	38.16	6.58	0.005	Extracellular and plasma membrane
AhAPX25	AH04G09830.1	Chr04 (16586332, 16594630, −)	1923	7	6	640	69.4	5.78	−0.138	Extracellular and plasma membrane
AhAPX26	AH04G09840.1	Chr04 (16603008, 16606152, −)	1113	4	3	370	39.73	5.72	−0.016	Extracellular
AhAPX27	AH04G09850.1	Chr04 (16611949, 16615189, −)	1077	4	3	358	38.56	5.74	−0.085	Extracellular
AhAPX28	AH04G09870.1	Chr04 (16648330, 16651554, −)	1080	4	3	359	38.83	7.51	−0.154	Extracellular
AhAPX29	AH04G10990.1	Chr04 (20506854, 20510294, +)	1047	3	2	348	38.82	5.58	−0.139	Extracellular and plasma membrane
AhAPX30	AH04G12400.1	Chr04 (28356898, 28358984, −)	990	4	3	329	36	7.58	−0.1	Extracellular
AhAPX31	AH04G06960.1	Chr04 (8749652, 8755948, +)	999	4	3	332	36	5.85	−0.117	Extracellular
AhAPX32	AH05G33570.1	Chr05 (109243748, 109247060, +)	1032	4	3	343	37.89	5.3	0.039	Plasma membrane
AhAPX33	AH05G34100.1	Chr05 (110343093, 110344607, −)	753	2	1	250	27.34	7.04	−0.191	Cytoplasmic
AhAPX34	AH05G02820.1	Chr05 (2952742, 2957237, +)	849	9	8	282	31.57	7.72	−0.496	Cytoplasmic
AhAPX35	AH05G12980.1	Chr05 (33401595, 33403392, −)	1269	2	1	422	45.9	5.21	−0.302	Cytoplasmic, nuclear, and extracellular
AhAPX36	AH05G03640.1	Chr05 (3964114, 3966683, +)	1047	4	3	348	39.09	5.89	−0.224	Extracellular
AhAPX37	AH05G04730.1	Chr05 (5512010, 5518889, −)	984	4	3	327	35.78	9.05	−0.147	Extracellular
AhAPX38	AH05G05760.1	Chr05 (7138559, 7139891, −)	984	4	3	327	35.88	6.42	0	Extracellular
AhAPX39	AH05G21680.1	Chr05 (87703778, 87704768, +)	645	3	2	214	23.47	5.95	−0.169	Extracellular

(Continued)

TABLE 1 | (Continued)

Gene name	Gene ID	Genomic region	CDS length (bp)	Exon	Intron	Protein length (aa)	MW (KDa)	PI	GRAVY	Subcellular localization
AhAPX40	AH05G21770.1	Chr05 (87831257, 87833413, –)	984	4	3	327	36	5.5	−0.127	Extracellular
AhAPX41	AH06G24710.1	Chr06 (101560772, 101566207, +)	990	3	2	329	35.4	5.31	−0.142	Extracellular and chloroplast
AhAPX42	AH06G24750.1	Chr06 (101678350, 101681066, –)	978	3	2	325	35.12	5.87	−0.095	Extracellular
AhAPX43	AH06G26990.1	Chr06 (106045942, 106046919, –)	981	1	0	326	35.92	8.33	−0.187	Extracellular and chloroplast
AhAPX44	AH06G12580.1	Chr06 (17096141, 17097919, –)	1050	4	3	349	38.3	9.06	−0.146	Extracellular
AhAPX45	AH06G12600.1	Chr06 (17107249, 17113857, –)	1923	16	15	640	70.66	8.94	−0.077	Chloroplast
AhAPX46	AH06G12640.1	Chr06 (17206186, 17208105, +)	1047	4	3	348	38	9.26	−0.121	Extracellular
AhAPX47	AH06G13400.1	Chr06 (18468981, 18470093, –)	957	3	2	318	34.52	8.79	−0.068	Extracellular
AhAPX48	AH06G00870.1	Chr06 (2535291, 2536767, –)	981	4	3	326	34.46	5.77	−0.012	Extracellular
AhAPX49	AH06G20810.1	Chr06 (88751346, 88752854, –)	954	2	1	317	34.17	9.07	−0.038	Extracellular
AhAPX50	AH06G20840.1	Chr06 (88866272, 88866907, –)	639	1	0	212	22.93	6.82	0.017	Chloroplast
AhAPX51	AH07G12530.1	Chr07 (18527530, 18532254, –)	972	4	3	323	35	9.76	−0.198	Extracellular and mitochondrial
AhAPX52	AH07G12560.1	Chr07 (18594967, 18601313, +)	1005	3	2	334	36.23	5.8	−0.22	Extracellular
AhAPX53	AH07G12590.1	Chr07 (18635964, 18639438, –)	900	4	3	299	32.1	6.41	0.088	Plasma membrane
AhAPX54	AH07G16820.1	Chr07 (44801964, 44806304, +)	1035	3	2	344	38.1	8.78	−0.11	Plasma membrane
AhAPX55	AH07G19820.1	Chr07 (62509939, 62515927, –)	1065	11	10	354	38.47	8.59	−0.324	Mitochondrial
AhAPX56	AH07G22100.1	Chr07 (73486525, 73488901, –)	1221	4	3	406	45.08	5.58	−0.359	Nuclear, extracellular, and plasma membrane
AhAPX57	AH07G07450.1	Chr07 (8286104, 8288644, –)	975	4	3	324	34.37	8.54	−0.083	Extracellular
AhAPX58	AH07G07460.1	Chr07 (8308573, 8309778, +)	762	4	3	253	27.57	8.83	−0.272	Extracellular and mitochondrial
AhAPX59	AH08G05850.1	Chr08 (10750010, 10755089, +)	1338	12	11	445	48.75	8.67	−0.428	Chloroplast
AhAPX60	AH08G13980.1	Chr08 (28333679, 28334962, –)	756	7	6	251	27.75	5.39	−0.48	Cytoplasmic
AhAPX61	AH08G15100.1	Chr08 (29841553, 29842344, –)	795	1	0	264	28.8	4.85	−0.335	Nuclear and cytoplasmic
AhAPX62	AH08G16780.1	Chr08 (31925820, 31927225, +)	984	4	3	327	35.85	8.93	−0.108	Extracellular
AhAPX63	AH08G19120.1	Chr08 (35244506, 35247372, +)	975	3	2	324	34.42	8.75	−0.044	Extracellular
AhAPX64	AH08G26960.1	Chr08 (47233841, 47238063, –)	993	10	9	330	35.63	8.42	−0.221	Chloroplast
AhAPX65	AH09G23660.1	Chr09 (106807615, 106809134, +)	984	2	1	327	35.95	8.06	−0.046	Extracellular and mitochondrial
AhAPX66	AH09G31660.1	Chr09 (116756835, 116759702, –)	984	4	3	327	35.92	6.09	−0.202	Extracellular
AhAPX67	AH09G08990.1	Chr09 (12467446, 12469586, +)	1011	4	3	336	36	9.22	−0.113	Nuclear and plasma membrane
AhAPX68	AH09G11440.1	Chr09 (19596211, 19598370, –)	1008	2	1	335	36.05	8.1	−0.094	Chloroplast and extracellular
AhAPX69	AH09G02450.1	Chr09 (2707377, 2709690, +)	1365	4	3	454	50.07	4.69	−0.35	Nuclear and plasma membrane
AhAPX70	AH09G19280.1	Chr09 (84644615, 84652197, +)	858	4	3	285	31.31	8.41	−0.263	Chloroplast
AhAPX71	AH09G20940.1	Chr09 (95646878, 95647778, –)	327	3	2	108	11.59	9.34	−0.157	Extracellular
AhAPX72	AH10G22530.1	Chr10 (100608918, 100612037, –)	1038	3	2	345	38.57	5.47	−0.136	Cytoplasmic

(Continued)

TABLE 1 | (Continued)

Gene name	Gene ID	Genomic region	CDS length (bp)	Exon	Intron	Protein length (aa)	MW (KDa)	PI	GRAVY	Subcellular localization
AhAPX73	AH10G28820.1	Chr10 (111234752, 111235885, –)	969	2	1	322	35.56	6.6	−0.064	Plasma membrane
AhAPX74	AH10G28830.1	Chr10 (111237536, 111239429, –)	975	3	2	324	35	5.98	0.028	Plasma membrane
AhAPX75	AH10G10440.1	Chr10 (17084135, 17085775, +)	966	4	3	321	35.11	9.49	−0.117	Mitochondrial
AhAPX76	AH10G05800.1	Chr10 (5516527, 5517924, –)	981	3	2	326	34.81	7.54	−0.036	Extracellular
AhAPX77	AH10G05810.1	Chr10 (5525856, 5527195, +)	996	2	1	331	35.55	8.98	−0.037	Extracellular
AhAPX78	AH10G06100.1	Chr10 (5774246, 5774909, –)	594	2	1	197	21	5.61	0.36	Plasma membrane and extracellular
AhAPX79	AH10G17560.1	Chr10 (81389354, 81391402, +)	957	3	2	318	3.85	9.4	−0.17	Extracellular
AhAPX80	AH10G20050.1	Chr10 (93192984, 93194610, +)	972	4	3	323	34.97	5.46	0.043	Plasma membrane
AhAPX81	AH10G21960.1	Chr10 (99235900, 99237538, +)	654	3	2	217	23.87	5.29	0.004	Plasma membrane
AhAPX82	AH11G28810.1	Chr11 (138798034, 138799289, +)	1011	4	3	336	37.9	8.48	−0.37	Nuclear
AhAPX83	AH11G31650.1	Chr11 (143323830, 143325073, +)	999	4	3	332	35.72	4.41	−0.172	Extracellular
AhAPX84	AH11G35510.1	Chr11 (148378457, 148381103, –)	885	3	2	294	32.16	9.23	−0.199	Extracellular
AhAPX85	AH11G36340.1	Chr11 (149098252, 149100518, –)	987	4	3	328	35.31	6.07	0.007	Extracellular
AhAPX86	AH11G11550.1	Chr11 (24493194, 24496183, +)	981	4	3	326	35.26	8.88	−0.057	Extracellular
AhAPX87	AH11G11700.1	Chr11 (25189097, 25190336, +)	687	3	2	228	24.68	4.81	−0.188	Extracellular
AhAPX88	AH11G02890.1	Chr11 (3085958, 3089759, –)	984	4	3	327	35.36	8.91	−0.135	Extracellular
AhAPX89	AH11G02910.1	Chr11 (3130507, 3135477, +)	1020	3	2	339	37.34	9.07	−0.284	Extracellular
AhAPX90	AH11G02940.1	Chr11 (3154813, 3157814, +)	858	3	2	285	31.1	9.36	−0.12	Extracellular
AhAPX91	AH11G02950.1	Chr11 (3166698, 3169834, –)	888	5	4	295	31.26	5.06	−0.145	Extracellular
AhAPX92	AH11G14080.1	Chr11 (38404886, 38409314, –)	1404	12	11	467	52.19	9.02	−0.453	Nuclear
AhAPX93	AH12G26730.1	Chr12 (108404606, 108406854, +)	975	4	3	324	35.2	8.28	−0.002	Extracellular
AhAPX94	AH12G26740.1	Chr12 (108408697, 108410986, +)	990	3	2	329	36.09	8.8	−0.234	Extracellular, mitochondrial and chloroplast
AhAPX95	AH12G26750.1	Chr12 (108428068, 108430589, +)	987	3	2	328	35.84	5.66	−0.264	Extracellular
AhAPX96	AH12G38300.1	Chr12 (122043858, 122045120, +)	996	3	2	331	37.38	6.26	−0.412	Extracellular
AhAPX97	AH13G48270.1	Chr13 (139486821, 139487952, +)	966	3	2	321	34	6.51	−0.101	Extracellular
AhAPX98	AH13G58440.1	Chr13 (149092750, 149095384, +)	975	3	2	324	35	5.88	0.011	Plasma membrane
AhAPX99	AH13G58450.1	Chr13 (149097506, 149098640, +)	969	2	1	322	35.33	6.31	−0.038	Extracellular
AhAPX100	AH13G15620.1	Chr13 (18204851, 18207371, +)	978	4	3	325	35.49	8.05	−0.013	Extracellular and plasma membrane
AhAPX101	AH13G03790.1	Chr13 (3974837, 3976803, –)	756	9	8	251	27	5.52	−0.319	Cytoplasmic
AhAPX102	AH13G08510.1	Chr13 (8737422, 8740756, +)	867	9	8	288	31.66	6.67	−0.311	Cytoplasmic
AhAPX103	AH13G09650.1	Chr13 (9945748, 9947398, –)	978	4	3	325	34.5	8.71	0.015	Extracellular
AhAPX104	AH14G24560.1	Chr14 (102202325, 102204136, +)	984	4	3	327	35.79	8.44	−0.154	Extracellular
AhAPX105	AH14G25410.1	Chr14 (105306662, 105308874, –)	924	4	3	307	32.74	5	−0.086	Extracellular
AhAPX106	AH14G25420.1	Chr14 (105316704, 105318852, –)	954	4	3	317	33.51	8.05	−0.034	Extracellular
AhAPX107	AH14G25430.1	Chr14 (105327285, 105329671, –)	957	4	3	318	33.64	8.51	−0.084	Extracellular
AhAPX108	AH14G08400.1	Chr14 (10636078, 10640476, +)	999	4	3	332	36.11	5.77	−0.137	Extracellular
AhAPX109	AH14G08420.1	Chr14 (10696309, 10699909, +)	1068	4	3	355	38.31	6.44	−0.153	Extracellular
AhAPX110	AH14G08430.1	Chr14 (10719836, 10722950, +)	1074	4	3	357	38.44	5.74	−0.075	Extracellular
AhAPX111	AH14G08440.1	Chr14 (10740576, 10743027, +)	1077	4	3	358	38.25	5.57	0.027	Extracellular
AhAPX112	AH14G08450.1	Chr14 (10751673, 10756427, +)	1068	4	3	355	38	4.99	−0.048	Extracellular
AhAPX113	AH14G08480.1	Chr14 (10795498, 10798919, +)	1068	4	3	355	38.14	6.2	−0.005	Extracellular
AhAPX114	AH14G08550.1	Chr14 (11049580, 11052270, –)	927	4	3	308	33.87	8.05	−0.041	Extracellular

(Continued)

TABLE 1 | (Continued)

Gene name	Gene ID	Genomic region	CDS length (bp)	Exon	Intron	Protein length (aa)	MW (KDa)	PI	GRAVY	Subcellular localization
AhAPX115	AH14G13430.1	Chr14 (22102438, 22105949, +)	1047	3	2	348	38.8	5.68	−0.149	Extracellular and plasma membrane
AhAPX116	AH14G16980.1	Chr14 (39854809, 39855923, +)	570	3	2	189	20.65	6.7	0.287	Extracellular and plasma membrane
AhAPX117	AH14G16990.1	Chr14 (39859734, 39860093, +)	363	1	0	120	13.39	9.03	−0.37	Extracellular
AhAPX118	AH14G21760.1	Chr14 (89731359, 89733140, −)	909	5	4	302	32.95	8.35	−0.201	Extracellular
AhAPX119	AH15G18730.1	Chr15 (105800589, 105804751, −)	1032	4	3	343	37.88	5.3	0.024	Plasma membrane
AhAPX120	AH15G00780.1	Chr15 (1195384, 1202015, −)	984	4	3	327	35.78	9.05	−0.147	Extracellular
AhAPX121	AH15G33980.1	Chr15 (148489966, 148492117, +)	984	4	3	327	36.17	5.88	−0.164	Extracellular and nuclear
AhAPX122	AH15G33990.1	Chr15 (148500369, 148501868, +)	705	4	3	234	25.5	4.8	−0.226	Cytoplasmic and chloroplast
AhAPX123	AH15G34130.1	Chr15 (148706618, 148708110, −)	834	5	4	277	30.66	6.22	−0.226	Extracellular and plasma membrane
AhAPX124	AH15G35170.1	Chr15 (149938106, 149940460, −)	669	3	2	222	24.22	7.67	−0.021	Extracellular
AhAPX125	AH15G37650.1	Chr15 (152607618, 152611276, −)	1092	3	2	363	40.13	5.51	−0.222	Extracellular
AhAPX126	AH15G09760.1	Chr15 (17115019, 17116810, +)	1257	2	1	418	45.61	5.4	−0.337	Extracellular, cytoplasmic and nuclear
AhAPX127	AH15G01790.1	Chr15 (3022442, 3024001, −)	984	4	3	327	36	6.87	−0.042	Extracellular
AhAPX128	AH16G05890.1	Chr16 (10586280, 10589926, −)	987	4	3	328	35.89	7.97	−0.131	Extracellular
AhAPX129	AH16G06030.1	Chr16 (10824424, 10825859, +)	882	4	3	293	32.28	8.53	−0.268	Extracellular
AhAPX130	AH16G25780.1	Chr16 (114921710, 114923167, −)	954	2	1	317	33.99	8.98	−0.027	Extracellular
AhAPX131	AH16G25800.1	Chr16 (115100883, 115101305, −)	426	1	0	141	15.52	6.28	−0.05	Extracellular, cytoplasmic and chloroplast
AhAPX132	AH16G30440.1	Chr16 (129635392, 129640099, +)	990	3	2	329	35.36	5.32	−0.127	Extracellular and chloroplast
AhAPX133	AH16G30490.1	Chr16 (129750891, 129753522, −)	975	3	2	324	34.81	5.87	−0.047	Extracellular
AhAPX134	AH16G33620.1	Chr16 (135979748, 135980725, −)	981	1	0	326	35.95	8.69	−0.161	Extracellular
AhAPX135	AH16G03520.1	Chr16 (7153751, 7155209, −)	981	4	3	326	34.38	5.31	−0.009	Extracellular
AhAPX136	AH16G01030.1	Chr16 (993418, 995239, +)	1050	4	3	349	38.29	9.17	−0.139	Extracellular
AhAPX137	AH17G30310.1	Chr17 (125992323, 125997218, −)	1338	12	11	445	48.73	8.8	−0.44	Chloroplast
AhAPX138	AH17G11990.1	Chr17 (20654955, 20659787, −)	972	4	3	323	34.93	9.74	−0.18	Extracellular
AhAPX139	AH17G12030.1	Chr17 (20764144, 20766484, +)	735	2	1	244	26.45	6.81	−0.317	Extracellular
AhAPX140	AH17G18150.1	Chr17 (49822929, 49829110, +)	1068	11	10	355	38.64	8.79	−0.338	Mitochondrial
AhAPX141	AH17G06310.1	Chr17 (7780769, 7782202, −)	963	4	3	320	34.92	8.65	−0.145	Extracellular
AhAPX142	AH17G06350.1	Chr17 (7839321, 7842337, +)	966	4	3	321	34	8.54	−0.113	Extracellular
AhAPX143	AH18G23730.1	Chr18 (103745127, 103747854, +)	1014	3	2	337	37.31	9.13	−0.136	Mitochondrial and plasma membrane
AhAPX144	AH18G10570.1	Chr18 (14253327, 14256241, +)	972	3	2	323	34.3	8.75	−0.044	Extracellular
AhAPX145	AH18G15530.1	Chr18 (26788797, 26795823, −)	1416	16	15	471	52.82	9	−0.639	Nuclear
AhAPX146	AH18G05400.1	Chr18 (5046262, 5048240, −)	969	2	1	322	35.34	5.8	−0.104	Plasma membrane
AhAPX147	AH18G07180.1	Chr18 (7610724, 7612104, +)	987	4	3	328	35.93	8.82	−0.101	Extracellular
AhAPX148	AH18G22460.1	Chr18 (92176526, 92178893, +)	1218	4	3	405	45.05	5.81	−0.101	Extracellular, nuclear and plasma membrane

(Continued)

TABLE 1 | (Continued)

Gene name	Gene ID	Genomic region	CDS length (bp)	Exon	Intron	Protein length (aa)	MW (KDa)	PI	GRAVY	Subcellular localization
AhAPX149	AH19G24230.1	Chr19 (108739539, 108750043, –)	996	4	3	331	36.82	6.95	–0.132	Extracellular
AhAPX150	AH19G26520.1	Chr19 (124514590, 124517216, –)	996	4	3	331	40.26	7.97	0	Extracellular and chloroplast
AhAPX151	AH19G29790.1	Chr19 (138198709, 138200248, +)	984	2	1	327	35.98	8.06	–0.054	Extracellular and mitochondrial
AhAPX152	AH19G36370.1	Chr19 (152526370, 152529191, +)	984	4	3	327	36.19	5.9	–0.225	Extracellular and nuclear
AhAPX153	AH19G42570.1	Chr19 (158270903, 158272107, –)	975	3	2	324	35.69	9.04	–0.179	Extracellular
AhAPX154	AH19G11940.1	Chr19 (16033083, 16035651, +)	1014	4	3	337	36.06	8.91	–0.113	Extracellular and plasma membrane
AhAPX155	AH19G14960.1	Chr19 (24411814, 24415355, –)	1278	3	2	425	46.49	6.47	–0.117	Chloroplast
AhAPX156	AH19G03800.1	Chr19 (3648102, 3650393, +)	1365	4	3	454	49.95	4.72	–0.351	Nuclear
AhAPX157	AH20G22440.1	Chr20 (100242945, 100244252, –)	987	4	3	328	35.74	6.17	–0.213	Extracellular and nuclear
AhAPX158	AH20G23580.1	Chr20 (107122955, 107124841, +)	957	3	2	318	33.85	9.4	–0.173	Extracellular
AhAPX159	AH20G08720.1	Chr20 (10757292, 10758717, –)	981	3	2	326	34.71	6.07	–0.028	Extracellular
AhAPX160	AH20G08730.1	Chr20 (10773674, 10775017, +)	999	2	1	332	35.59	8.98	–0.023	Extracellular
AhAPX161	AH20G09010.1	Chr20 (11124003, 11124708, –)	636	2	1	211	22.75	4.93	0.392	Plasma membrane
AhAPX162	AH20G26300.1	Chr20 (119159975, 119161601, +)	972	2	1	323	35	5.32	0.067	Plasma membrane
AhAPX163	AH20G28750.1	Chr20 (126510516, 126511240, +)	465	2	1	154	17	6.4	–0.372	Nuclear
AhAPX164	AH20G28770.1	Chr20 (126544791, 126546815, +)	927	4	3	308	33.85	4.89	–0.132	Extracellular and cytoplasmic
AhAPX165	AH20G29320.1	Chr20 (128237247, 128240109, –)	1038	3	2	345	38.54	5.38	–0.138	Cytoplasmic
AhAPX166	AH20G14810.1	Chr20 (25055084, 25056732, +)	969	4	3	322	35.15	9.54	–0.139	Mitochondrial

In the genomic position, the positive (+) and negative (–) sign shows the presence of a gene on the positive and negative strand of that specific marker correspondingly. MW, molecular weight; PI, isoelectric points; bp, base pair; aa, amino acids.

showed a greater phylogenetic network with the AdAPXs and AiAPXs in each group.

Insights Into Synteny and Collinearity of *APX* Genes

Gene duplications (i.e., tandem and segmental) are thought to be the main factors in supporting the expansion and evolution of new gene families in plants (Cannon et al., 2004). Hence, gene duplication procedures were assessed between *AhAPXs, AdAPXs, AiAPXs,* and *AtAPXs* (**Supplementary Table 3**). The results of gene duplication study showed that there were 92 *AhAPX* gene pairs, and these pairs were unevenly mapped on different chromosomes (**Figure 3** and **Supplementary Table 3**). Mainly, chromosome 13 had a maximum number (i.e., 16) of *AhAPX* gene pairs, followed by chromosome 5 with 12 *AhAPX* gene pairs. The least number of gene pairs (i.e., two) was discovered on chromosome 12, and no gene pair was found on chromosome 2 (**Figure 3** and **Supplementary Table 3**). The results reveal that segmental duplications have contributed to the expansion of *AhAPX* genes in the cultivated peanut genome (**Supplementary Table 3**). Notably, no tandem duplicated gene pairs were identified.

Similarly, 10 duplicated gene pairs were detected between *AhAPX* and *AtAPX* (**Supplementary Figure 1** and **Supplementary Table 3**); 171 pairs between *AhAPX* and *AiAPX* (**Supplementary Figure 2** and **Supplementary Table 3**); and 160 pairs between *AhAPX* and *AdAPX* (**Supplementary Figure 3** and **Supplementary Table 3**). All these gene pairs were irregularly mapped on different chromosomes. Taken together, these conclusions explained that the duplication activities played a vital role in enlarging the *APX* genes between diploid and tetraploid parents. Further, it can also be concluded that *A. hypogea* might have lost some genes during genome evolution.

Collinearity analysis was carried out to review the evolutionary association of the *APX* genes between *A. hypogea, A. duranensis, A. ipaensis,* and *A. thaliana* (**Figure 4** and **Supplementary Table 3**). The results discovered a strong orthologous of *APX* genes among these four species (**Figure 4**). On the whole, several *A. hypogea* genes presented syntenic networks with different *AdAPX, AiAPX,* and *AtAPX* genes. Particularly, only one gene (*AhAPX14*) at chromosome Ah2

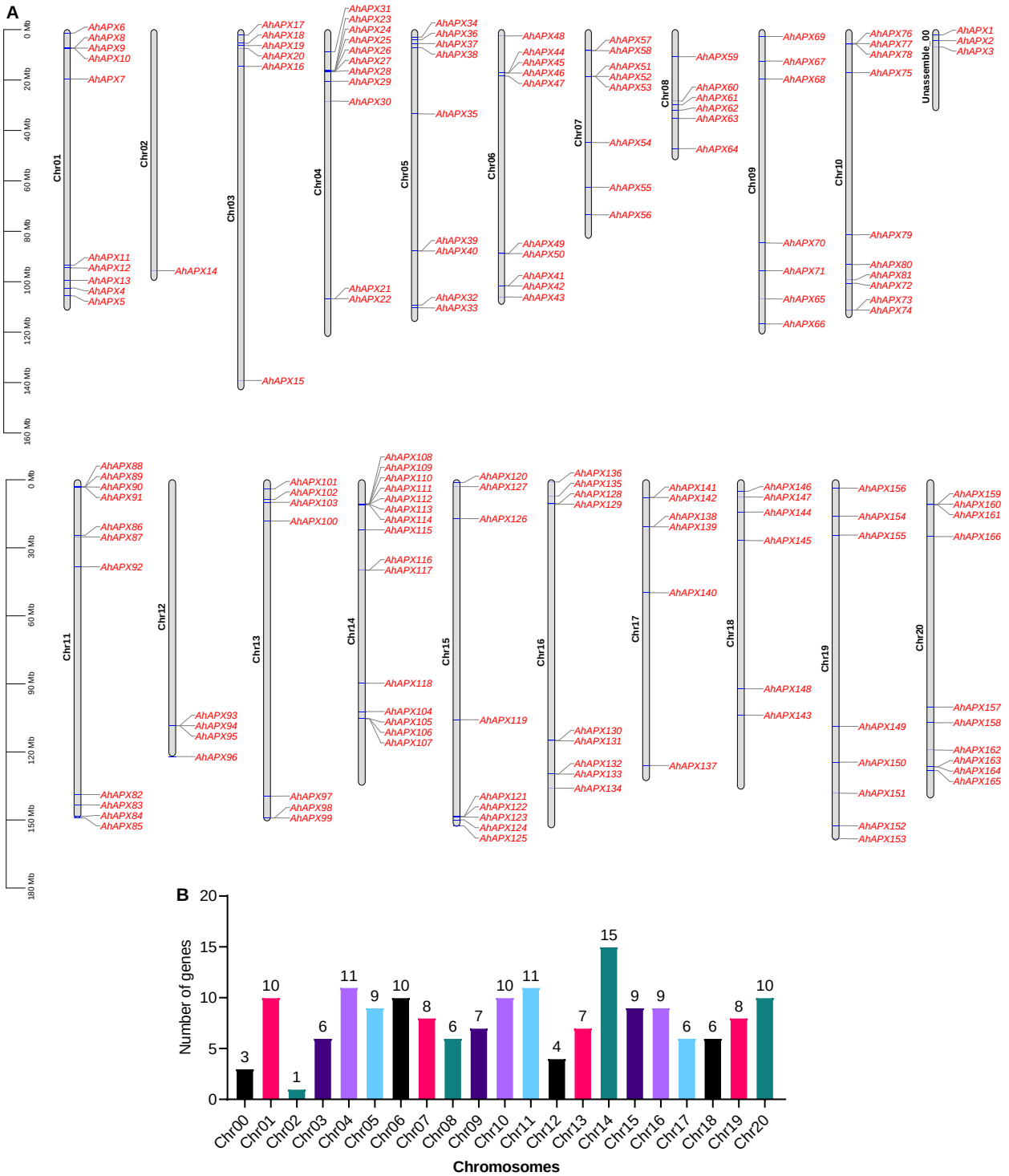

FIGURE 1 | Chromosomal mapping of *AhAPX* genes on *A. hypogea* genome. **(A)** Distribution map of *AhAPX* genes on 20 chromosomes, including one unassembled region. Representative chromosome numbers are shown on the left side of each bar. The scale on the left side represents the chromosomal distance and is in megabases (Mb). **(B)** Graph indicates the number of *AhAPX* genes mapped on each chromosome.

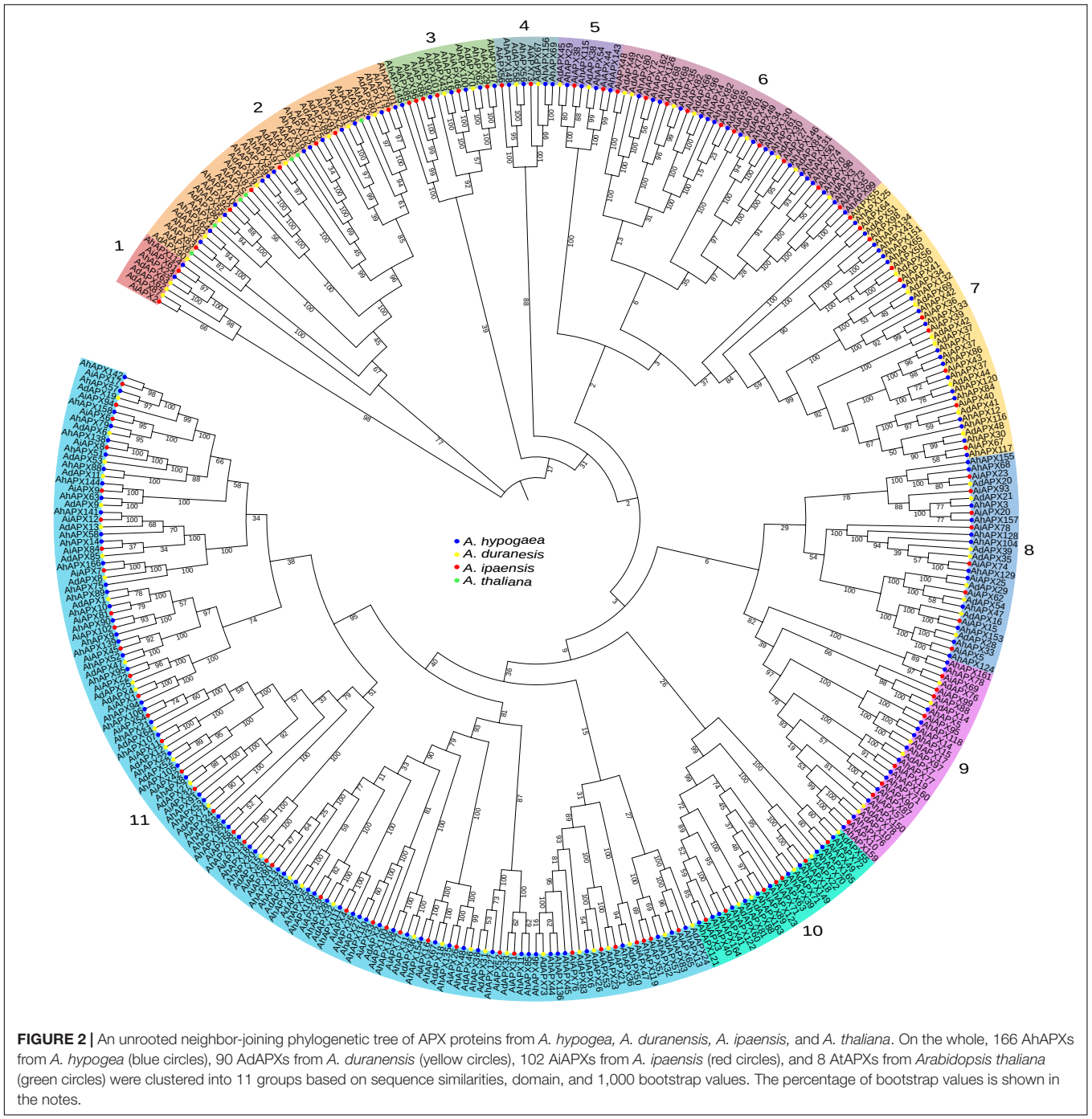

FIGURE 2 | An unrooted neighbor-joining phylogenetic tree of APX proteins from *A. hypogea, A. duranensis, A. ipaensis,* and *A. thaliana*. On the whole, 166 AhAPXs from *A. hypogea* (blue circles), 90 AdAPXs from *A. duranensis* (yellow circles), 102 AiAPXs from *A. ipaensis* (red circles), and 8 AtAPXs from *Arabidopsis thaliana* (green circles) were clustered into 11 groups based on sequence similarities, domain, and 1,000 bootstrap values. The percentage of bootstrap values is shown in the notes.

exhibited a syntenic connection with *AdAPX85* gene at chromosome Ad02 (**Figure 4** and **Supplementary Table 3**), while other homologous genes present on other *A. hypogea* chromosomes also showed a syntenic relationship with many *AdAPX*, *AiAPX* and *AtAPX* genes (**Figure 4** and **Supplementary Table 3**). These findings indicate that whole-genome or segmental duplication procedures are considered a main evolutionary force in the evolution of *AhAPX* genes in the peanut genome (**Figure 4** and **Supplementary Table 3**).

The Ka/Ks ratio is considered as a huge diagnostic marker in evaluating the sequence evolution in terms of selection pressures and duplication types (Hurst, 2002). Thus, to understand the evolutionary story of the *AhAPX*, the Ka, Ks, and Ka/Ks ratio was revealed (**Supplementary Table 3**). The dataset unveiled that all duplicated *AhAPX* gene pairs had a Ka/Ks ratio of <1

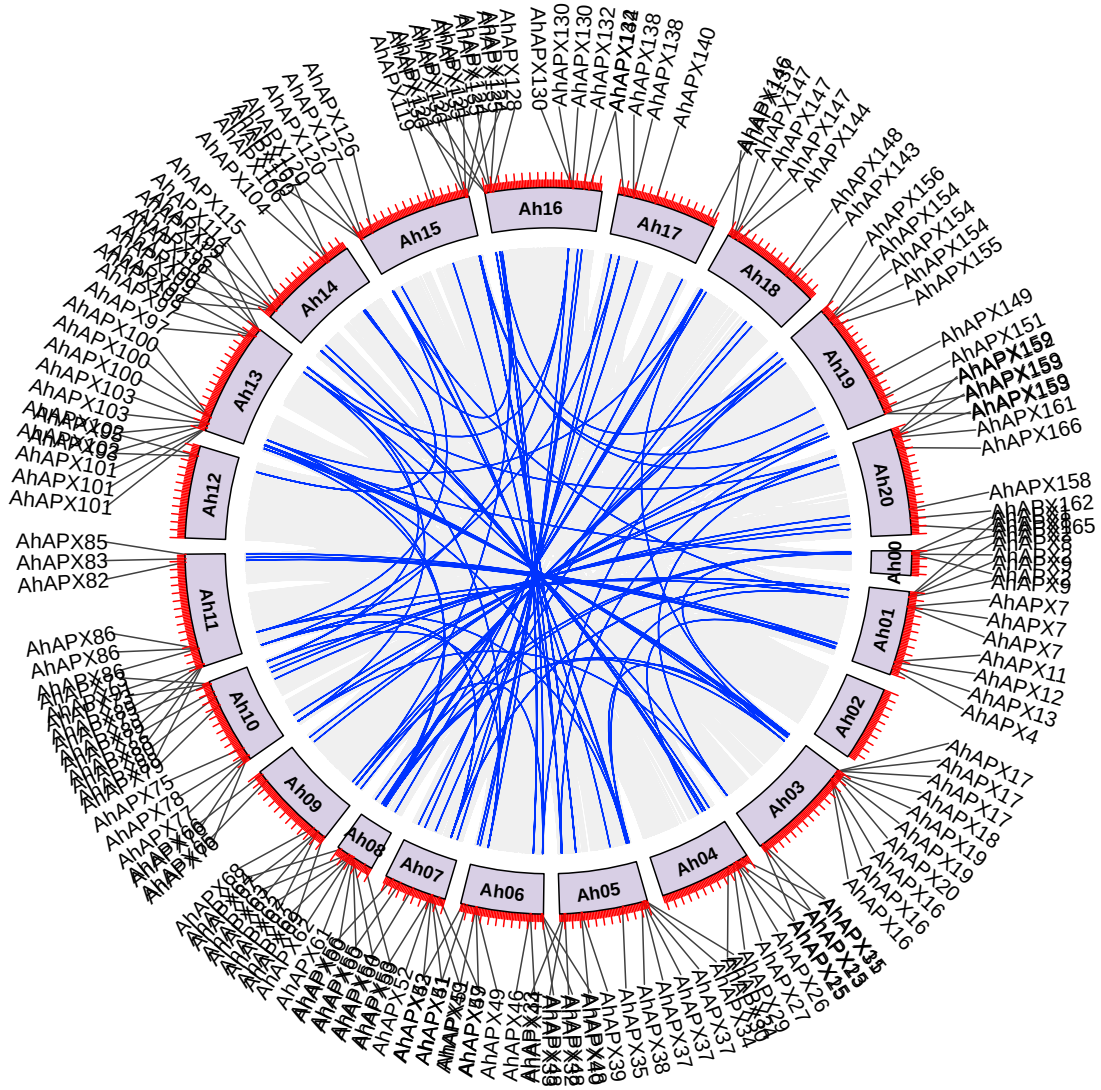

FIGURE 3 | Chromosomal positions and inter-chromosomal groups of duplicated *AhAPX* gene pairs. Gray lines in the background demonstrate all syntenic blocks in the *A. hypogea* genome, and the blue lines exhibit the segmental or tandem duplication network zones among *AhAPX* genes. The near location of *AhAPX* genes is marked with black lines outside with chromosome names.

(**Supplementary Table 3**), demonstrating that the *AhAPX* genes may have experienced strong purifying selective pressure and segmental duplications throughout the evolution procedure (**Supplementary Table 3**).

Insights Into Gene Structures and Conserved Motifs of *AhAPX* Genes

The exon-intron arrangements and conserved motifs of the *AhAPX* genes were analyzed to get insights into the advancement of the *APX* family genes in peanut genome (**Figure 5** and **Supplementary Table 4**). The outcomes revealed that the number of exons and introns varied from 16 to 1 and 0 to 15, respectively (**Figure 5B** and **Supplementary Table 10**). In short, 6 genes have 1 exon and zero intron; 13 genes have 2 exons and 1 intron; 5 genes have 3 exons and 2 introns; 18 genes have 2 exons and 1 intron; 41 genes have 3 exons and 2 introns; 81 genes have 4 exons and 3 introns; 3 genes have 5/7 exons and 4/6 introns; 5 genes have 9 exons and 8 introns; only 1 gene has 10 exons and 9 introns; 3 genes have 11/12 exons and 10/11 introns; and only 2 genes have a maximum number of exons (16) and introns (15) (**Figure 5B** and **Supplementary Table 10**). Above all, genes belonging to the same sub-tree almost had parallel structures apart from a few genes (**Figure 5B**). Among all genes, *AhAPX149* possess the longest structure, and only a few genes have a complex structure, such as *AhAPX17, AhAPX19, AhAPX34, AhAPX45, AhAPX55, AhAPX59, AhAPX64, AhAPX92, AhAPX101, AhAPX102,* and *AhAPX145* (**Figure 5B**). Exon loss or gain has been found during the evolution of *APX* family genes.

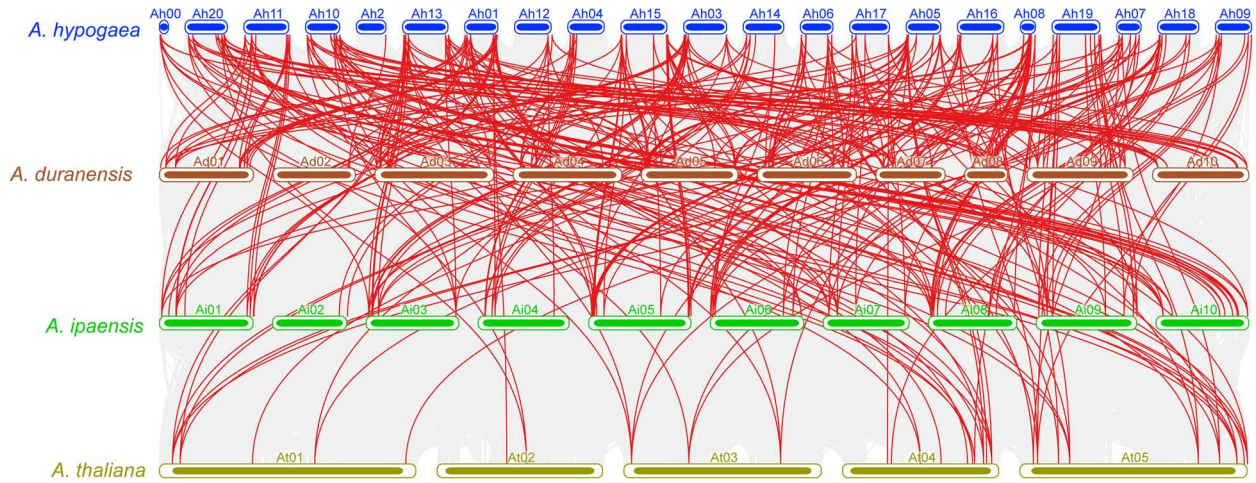

FIGURE 4 | Multiple collinearity analysis of *APX* genes between *A. hypogea, A. duranensis, A. ipaensis,* and *A. thaliana* chromosomes. Gray lines in the background specify the collinear blocks within *A. hypogea* and other three genomes, while the red lines highlight the syntenic *APX* orthologous gene pairs.

The results recommended that *APX* genes held a somewhat frequent exon-intron composition throughout the evolution of peanut genome. Furthermore, *AhAPX* gene participants inside a sub-tree had exceptionally corresponding gene structures, steady with their phylogenetic clusters.

The conserved motif of the *AhAPX* genes ranged from one (*AhAPX55/140*) to three (*AhAPX2/71/117/131*) (**Figure 5A**). In total, 10 conserved motifs were recognized, and their complete dataset, including motif names, sequences, width, and E-value, is given in **Supplementary Table 4**. Similar to gene structure, the motif distributions were also similar within the sub-trees (**Figure 5A**), while some motifs were found to be specific to some genes. For instance, some genes such as *AhAPX2/17/101/34/59/137* were limited to motifs 2, 3, and 10. While *AhAPX60* gene only contained motifs 3 and 10; AhAPX71 contained motifs 3, 8, and 9; AhAPX117 contained motifs 4, 6, and 10; AhAPX131 contained motifs 4, 9, and 10; and AhAPX71 contained motifs 3, 8, and 9 (**Figure 5A**). Almost all other motifs were present on all genes except in a few cases (**Figure 5A**). In summary, the consistency of gene organizations within sub-trees was credibly constant by appraising the conserved motif structures, gene structures, and phylogenetic relations, representing that the APX proteins have enormously well-sustained amino acid deposits and APX members belonging to the same tree may hold corresponding roles.

Cis-Elements: Key Players in the Promoter Regions of *AhAPX* Genes

To better understand the regulatory role of *AhAPX* genes toward peanut growth and development, and tolerance to abiotic stress and phytohormones treatment, *cis*-regulatory elements in the promoter of *AhAPX* were explored. The complete dataset of *cis*-elements is presented in **Supplementary Table 5**. We emphasized and recognized three categories of *cis*-elements, including abiotic stress-responsive, phytohormones responsive, and growth and development responsive elements (**Figures 6**, **7** and **Supplementary Table 5**). Mainly, six abiotic stress-responsive (drought, light, low temperature, wound, defense and stress, and anaerobic) elements were detected. These elements consist of I-box, ATCT-motif, Box 4, GT1-motif, GA-motif, etc. (light-responsive, 77%), ARE (13%), MBS (3%), TC-rich repeats (3%), LTR (3%), and WUN-motif (0.15%) (**Figures 7A,B** and **Supplementary Table 5**). Overall, results showed that most of the abiotic stress-related elements were predicted to be specific to some genes and unevenly distributed (**Figure 6** and **Supplementary Table 5**), indicating their defensive role against stress conditions.

Likewise, five phytohormone-responsive elements [methyl jasmonate (MeJA), abscisic acid, gibberellin, salicylic acid, and auxin] consist of CGTCA-motif/TGACG-motif (36%), ABRE (35%), P-box/TATC-box/GARE-motif (11%), TCA-element/SARE (11%), and AuxRR-core/TGA-element/TGA-box (7%) (**Figures 7C,D** and **Supplementary Table 5**). Some of the elements were found to be specific to some genes and unevenly distributed (**Figure 6** and **Supplementary Table 5**). These outcomes suggest that element-specific genes could be considered as candidate players for further functional studies to reveal their protective role under hormone treatments.

Moreover, five growth and development-related (zein metabolism, meristem expression, endosperm expression, circadian control, and cell cycle regulation) elements were discovered. These key elements include O_2-site (34%), CAT-box (31%), GCN4_motif/AACA_motif (17%), circadian (14%), and MSA-like (5%) (**Figures 7E,F** and **Supplementary Table 5**), suggesting their dynamic role in different growth and developmental stages of peanut. In a nutshell, these discoveries suggested that some of the key elements are widely and randomly distributed in some genes, while some of the elements are found to be specific to some genes. It can be concluded that the

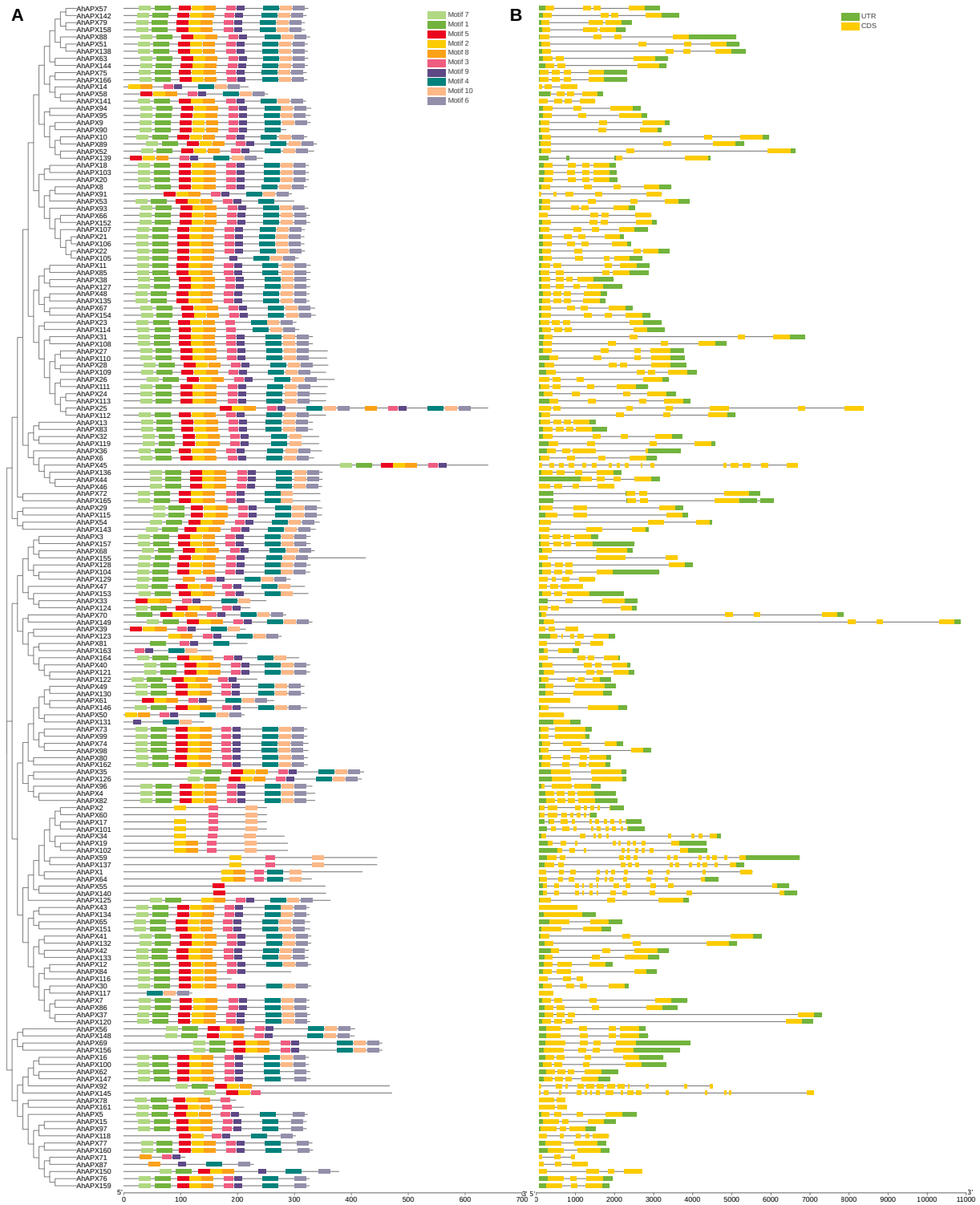

FIGURE 5 | The gene structure and motif analysis of the *AhAPX* genes. **(A)** Arrangements of predicted conserved motifs in *AhAPXs*. Unique color boxes exhibit individual motifs. **(B)** The gene structure of the *AhAPXs*. Light green color indicates the UTR regions; yellow color shows the CDS regions, and gray horizontal line displays the introns.

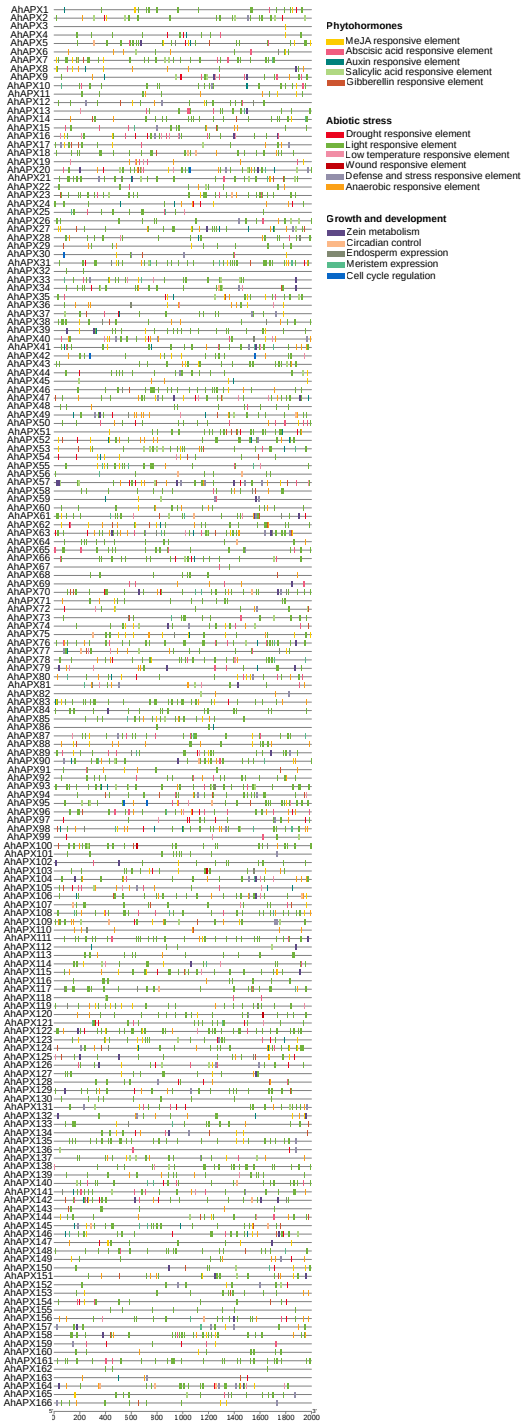

FIGURE 6 | Analysis of *cis*-regulatory elements in the *AhAPX* promoter regions. Diverse *cis*-elements with functional resemblance are represented by similar colors.

expression profiles of *AhAPX* genes may fluctuate under different developmental stages, phytohormone and abiotic stress conditions.

Genome-Wide Investigation of miRNAs Targeting *AhAPX* Genes

To better comprehend the miRNA-arbitrated post-transcriptional alteration of *AhAPX* genes, we identified 14 miRNAs targeting 33 genes (**Figure 8A** and **Supplementary Table 6**). These miRNAs belong to 12 different families. To give an overview, the miRNA-targeted sites of *AhAPX29* and *AhAPX147* are shown in **Figures 8B,C**, whereas the complete dataset of all miRNAs targeted sites/genes is provided in **Supplementary Table 6**. The results showed that ahy-miR159 and ahy-miR3513-3P targeted the most number (5) of genes. Three miRNAs, including ahy-miR3518, ahy-miR3520-3P, and ahy-miR3513-5P targeted four genes, followed by ahy-miR3520-5P that targeted three genes (*AhAPX38*, *AhAPX127*, and *AhAPX118*). While six miRNAs including ahy-miR3512, ahy-miR3510, ahy-miR167-3P, ahy-miR3514-5P, ahy-miR3509-3P, and ahy-miR3508 targeted two different genes individually. Notably, only two miRNAs (ahy-miR156b-5p and ahy-miR3516) targeted one gene, *AhAPX155* and *AhAPX128*, respectively (**Figure 8A** and **Supplementary Table 6**). Some common genes like *AhAPX29, AhAPX62, AhAPX115, AhAPX147, AhAPX74,* and *AhAPX98* are found to be targeted by more than one miRNA. Hence, the expression profiling of these predicted miRNAs and their targeted genes necessitates confirmation to oversee their biological roles in the cultivated peanut genome.

Transcription Factor Regulatory Network of *AhAPX* Genes

To get further insights into the regulatory role of transcription factors (TFs) in regulating the transcription of *AhAPX* genes, we identified 3,257 TFs in 162 *AhAPX* genes (**Figure 9** and **Supplementary Table 7**). The results showed that these TFs belong to 38 diverse TFs families, including AP2, ARF, B3, bHLH, bZIP, Dof, ERF, MYB, NAC, WRKY, HSF, GATA, etc. (**Figure 9** and **Supplementary Table 7**). The amplest TFs families were Dof (742 members), ERF (698 members), MYB (545 members), BBR-BPC (344 members), NAC (308 members), WRKY (238 members), GATA (223 members), MIKC_MADS (210 members), C2H2 (177 members), bHLH/bZIP (163 members), B3 (157 members), AP2 (154 members), and HSF (102 members) (**Figure 9B** and **Supplementary Table 7**). However, the least ample TFs families were ARR-B/RAV/SRS (2 members), followed by GrBP (4 members), S1Fa-like (6 members), SBP (7 members), C3H (8 members), etc. (**Figure 9B** and **Supplementary Table 7**). In contrast, other TFs families contained less than 100 members. Nearly, all 162 *AhAPX* genes were anticipated to be targeted by various TFs belonging to diverse families. For instance, *AhAPX150* gene was abundantly tarted by 314 TFs, followed by *AhAPX56* by 172 TFs, *AhAPX148* by 145 TFs, *AhAPX55* by 107 TFs, *AhAPX92* by 93 TFs, *AhAPX45* by 96 TFs., etc. (**Figure 9** and **Supplementary Table 7**). Some genes were nominally targeted, e.g., *AhAPX5/79/99* by 1 TF, *AhAPX83/90/93* by 2 TFs, *AhAPX9/15* by 3 TFs, *AhAPX7* by 4 TFs, *AhAPX8/70/80* by 5 TFs., etc. (**Figure 9** and

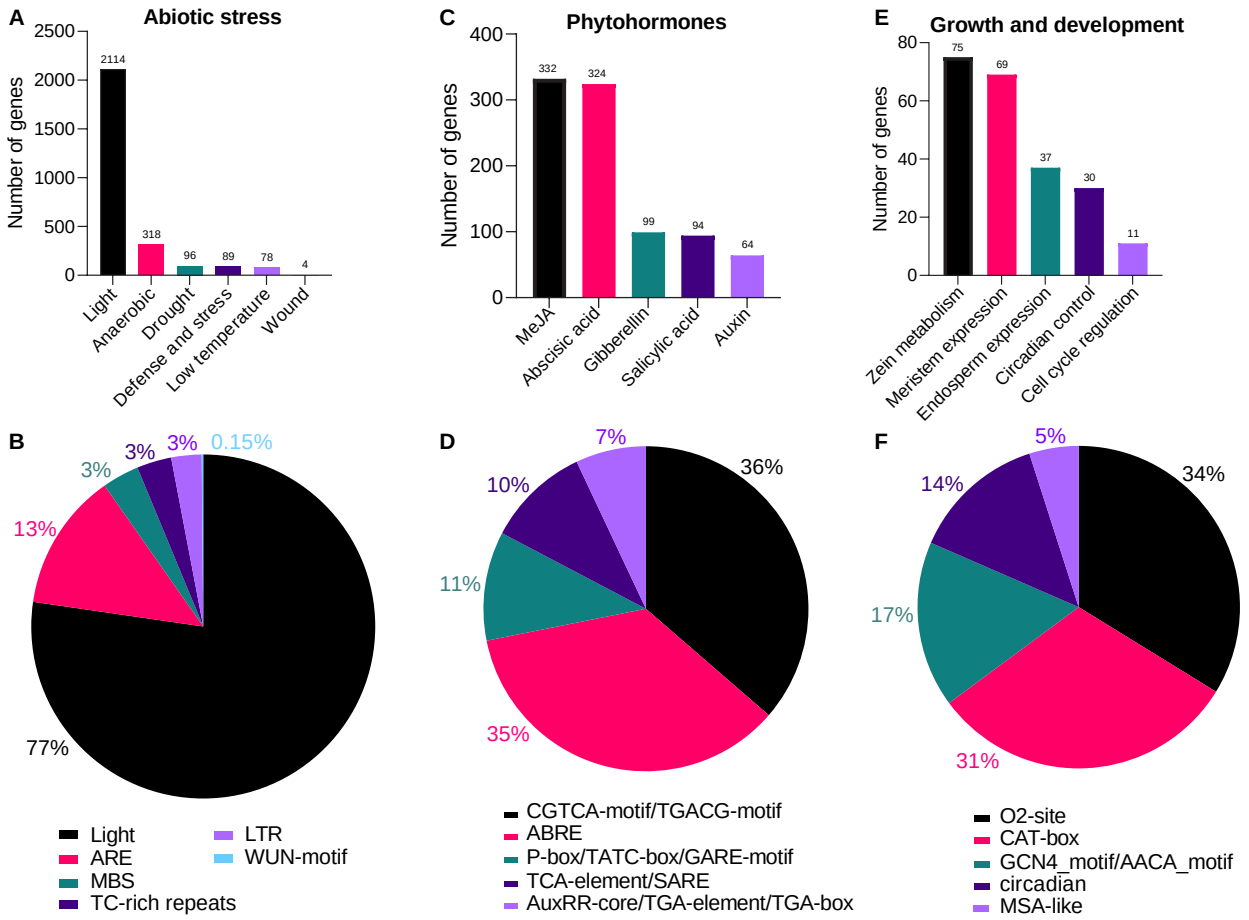

FIGURE 7 | *Cis*-regulatory elements in the *AhAPX* promoter regions. **(A,C,E)** The total number of *AhAPX* genes involved in abiotic stress, phytohormones, and growth and development categories of *cis*-elements. **(B,D,F)** The percentage (%) ratio of the several *cis*-elements from each category is shown in pie charts, i.e. **(B)** abiotic stress-responsive, **(D)** phytohormones responsive, and **(F)** plant growth and development responsive. Diverse colors signify different *cis*-acting elements and their ratio present in *AhAPX* genes.

Supplementary Table 7). Overall, these results showed that abiotic and phytohormone-related TFs could be engineered to develop improved peanut cultivars.

Gene Ontology and Kyoto Encyclopedia of Genes and Genomics Enrichment Analysis of *AhAPX* Genes

To advance our knowledge about the dynamic roles of *AhAPX* genes at molecular level, GO and KEGG enrichment analysis were performed (**Figure 10** and **Supplementary Table 8**). The GO annotation outcomes of biological process (BP), molecular function (MF), and cellular component (CC) classes presented quite a few substantially enriched terms (**Figure 10A** and **Supplementary Table 8**). For instance, in MF class, the highly enriched terms were cytochrome-c peroxidase activity (GO:0004130), oxidoreductase activity (GO:0016491), catalytic activity (GO:0003824), antioxidant activity (GO:0016209), and peroxidase activity (GO:0004601). In CC class, the most enriched terms were cell wall (GO:0005618), and cell junction (GO:0030054). Whereas in BP class, the highly enriched terms were cellular response to stimulus (GO:0051716), cellular detoxification (GO:1990748), response to chemical (GO:0042221), hydrogen peroxide catabolic process (GO:0042744), response to zinc ion (GO:0010043), modulation by symbiont of host defense response (GO:0052031), obsolete oxidation-reduction process (GO:0055114), detoxification (GO:0098754)., etc. (**Figure 10A** and **Supplementary Table 8**).

Furthermore, KEGG pathway enrichment study discovered six pathways participating in diverse functions of *AhAPX* genes (**Figure 10B** and **Supplementary Table 8**). The highly enriched pathways include biosynthesis of other secondary metabolites (B09110), metabolism (A09100), phenylpropanoid biosynthesis (00940), followed by ascorbate and aldarate metabolism (00053), glutathione metabolism (00480), and metabolism of other amino acids (B09106) (**Figure 10B** and **Supplementary Table 8**). Briefly, it can be concluded that GO and KEGG enrichment study validates the functional contribution of *AhAPX* genes in several cellular, molecular, and biological

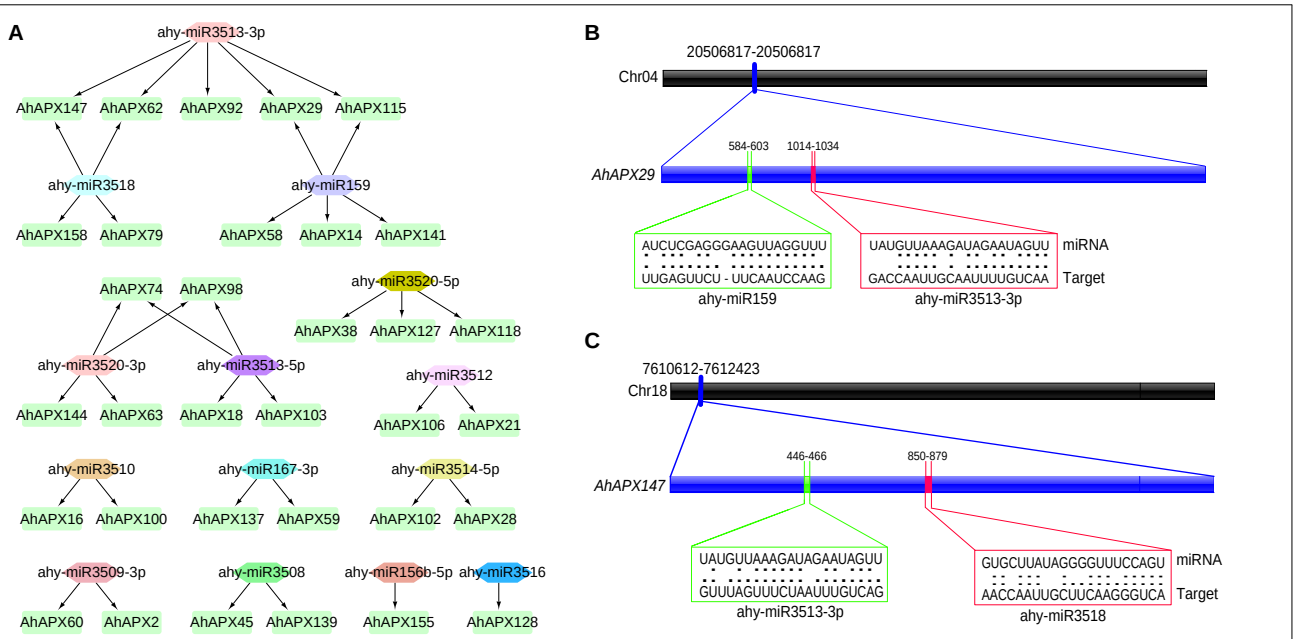

FIGURE 8 | miRNA targeting *AhAPX* genes. **(A)** Network map of projected miRNA targeting *AhAPX* genes. The green boxes correspond to *AhAPX* genes, and various color shapes indicate predicted miRNAs. **(B)** The graphic illustration indicates the *AhAPX29* gene is targeted by miRNAs (ahy-miR159 and ahy-miR3513-3p). **(C)** The graphic illustration shows the *AhAPX147* gene is targeted by miRNAs (ahy-miR3518 and ahy-miR3513-3p). Black thick bar indicates the chromosomal location of gene. Blue thick bar indicates the location of miRNAs on gene sequence. The RNA sequence of each complementary site from 5′ to 3′ and the predicted miRNA sequence from 3′ to 5′ are shown in the green and red line boxes. The complete dataset of predicted miRNAs is shown in **Supplementary Table 6**.

processes, that are associated with antioxidant defense systems, ROS scavenging, response to stresses, and biosynthesis of different metabolites.

Expression Profiling of *AhAPX* Genes at Diverse Developmental Tissues

The expression profiling of 166 *AhAPX* genes was observed in various tissues and organs, including embryo, cotyledon, testa, pericarp, peg, root and stem, root nodule, root tip, root, step tip, stem, leaf, and flower using openly available transcriptome dataset (**Supplementary Table 9**). Overall, the expression heatmap indicated that only a few genes were highly expressed in certain organs/tissues (**Figure 11** and **Supplementary Table 9**). For example, some genes including *AhAPX4, AhAPX7, AhAPX17, AhAPX19, AhAPX28, AhAPX42, AhAPX51, AhAPX76, AhAPX77, AhAPX82, AhAPX86, AhAPX101, AhAPX102, AhAPX130, AhAPX133,* and *AhAPX160* were highly expressed in almost all the organs/tissues (**Figure 11**). While some genes were found to be specific to some tissues like *AhAPX12* showed considerable expression in cotyledon, root and stem, root tip, and stem; *AhAPX109, AhAPX111,* and *AhAPX13* expressed in stem, roots and peg; *AhAPX135* expressed in pericarp; and *AhAPX138* expressed in cotyledon (**Figure 11**). Particularly, a few genes also exhibited modest expressions in a variety of tissues. On the whole, expression dataset shows that some particular genes may substantially participate in peanut growth and development. Hence, the functional characterization of these genes may perhaps be carried out in future studies.

Expression Profiling of *AhAPX* Genes Under Abiotic Stress and Hormones Treatments

To further study the contribution of all *AhAPX* genes toward abiotic and hormones stress tolerance in peanut, an openly available transcriptome dataset was used to evaluate the expression levels (**Figure 12** and **Supplementary Table 9**). Similar to tissue-specific trend, only a few genes showed higher expressions in both cold and drought stresses. For instance, *AhAPX4, AhAPX17, AhAPX19, AhAPX82, AhAPX101,* and *AhAPX102* were highly expressed under stress (cold and drought) and CK conditions. Likewise, some genes also showed moderate expression levels, such as *AhAPX27, AhAPX34, AhAPX51, AhAPX55, AhAPX59, AhAPX113, AhAPX137, AhAPX138, AhAPX140,* and *AhAPX157* under stress (cold and drought) and normal conditions. On the other hand, *AhAPX720, AhAPX21, AhAPX51, AhAPX77, AhAPX106, AhAPX130, AhAPX158,* and *AhAPX160* displayed considerable expression under cold stress compared to CK conditions (**Figure 12A**).

Under phytohormones treatments, *AhAPX4, AhAPX17, AhAPX55, AhAPX59, AhAPX82, AhAPX101, AhAPX102, AhAPX137,* and *AhAPX140* displayed significantly higher expression patterns throughout the treatments. In comparison

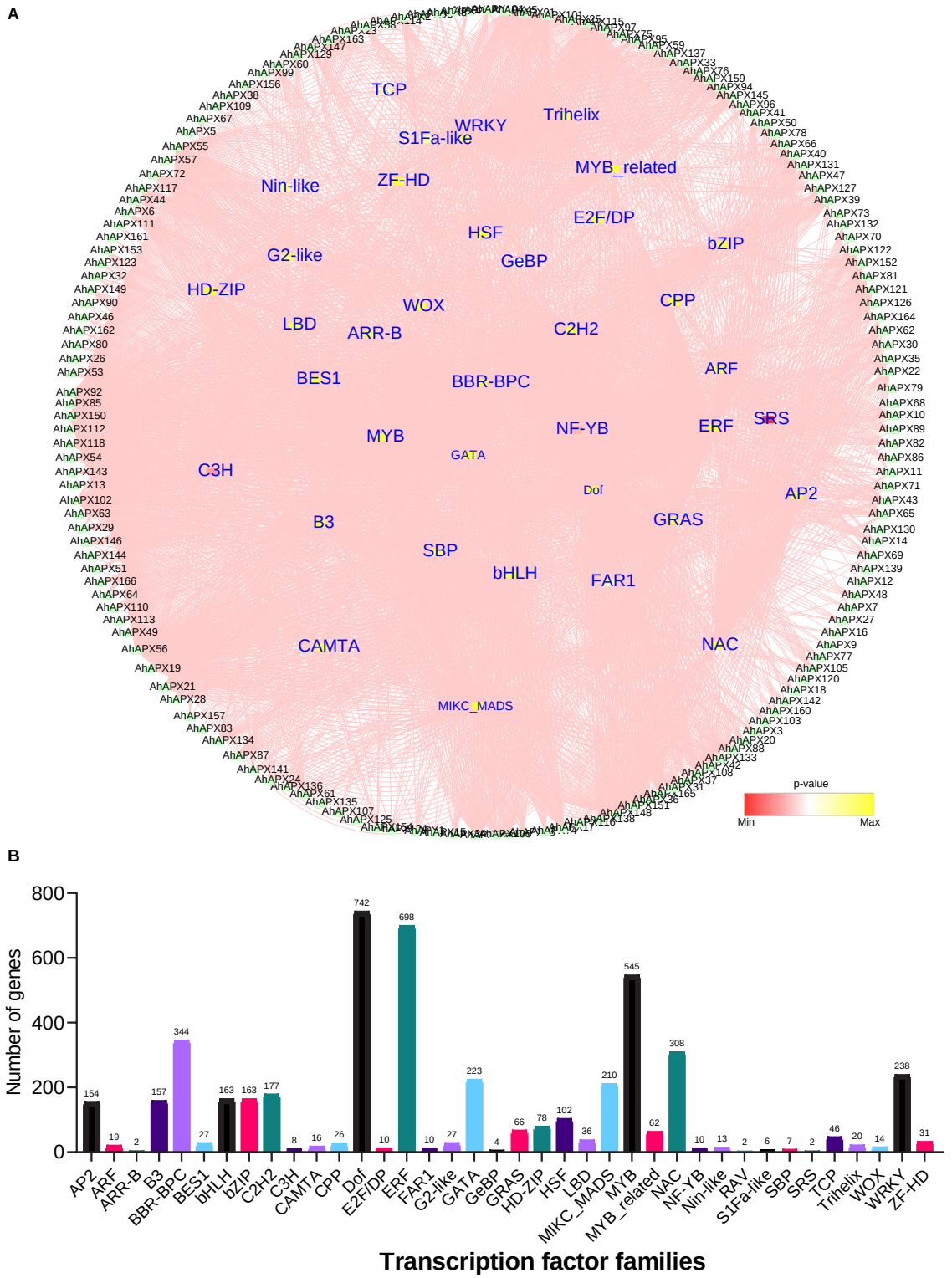

FIGURE 9 | The regulatory network of putative transcription factors of *AhAPX* genes. **(A)** Circular network of transcription factors. *AhAPX* genes are shown around the circle. The small inner circles denote the transcription factors, and their color pink to yellow represents the degree of interaction. **(B)** Graph indicates the number of *AhAPX* genes and their representative putative transcription factor families. The complete dataset of putative transcription factors is shown in **Supplementary Table 7**.

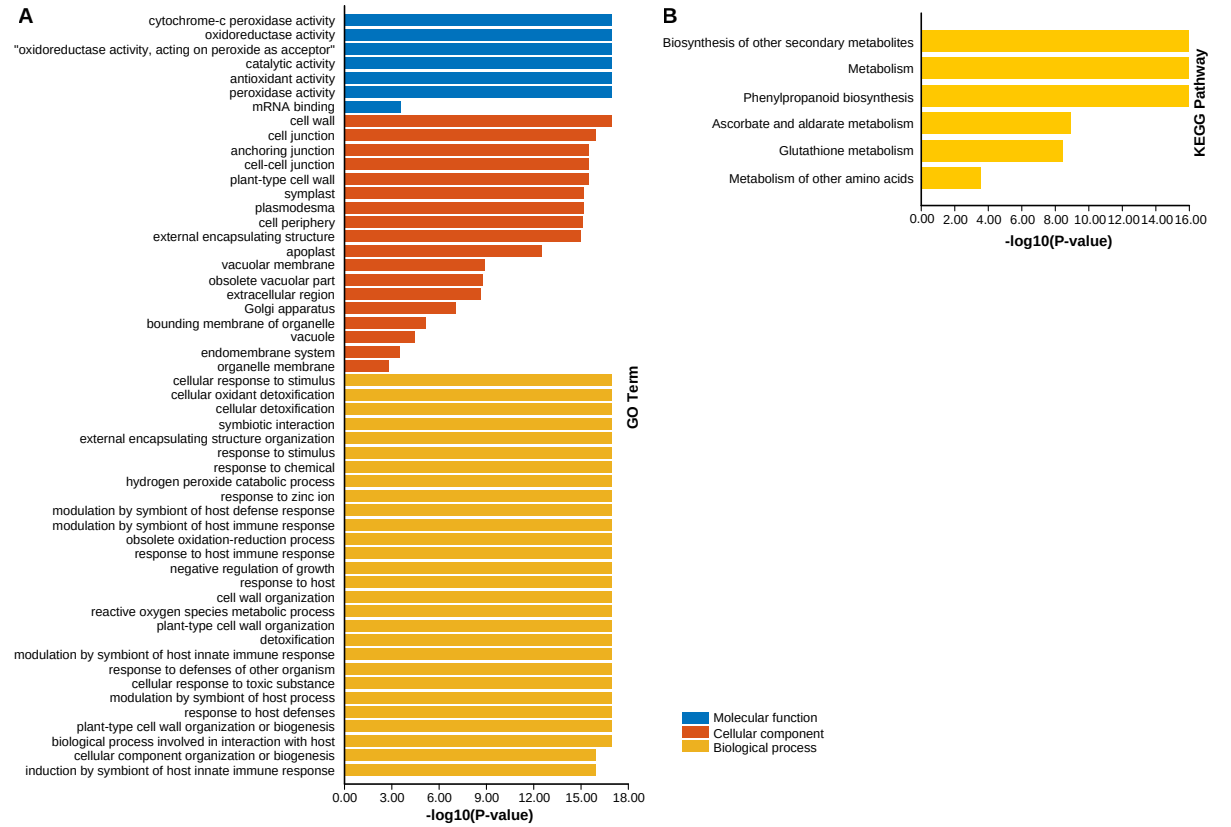

FIGURE 10 | Gene ontology (GO) and KEGG enrichment analysis of *AhAPX* genes. **(A)** The highly enriched GO terms from MF, CC, BP classifications in *AhAPX* genes. **(B)** The highly enriched KEGG pathways in *AhAPX* genes.

to CK, some genes are specifically expressed under certain hormones, such as *AhAPX21* under paclobutrazol, *AhAPX27* under ethylene and abscisic acid, *AhAPX51* under abscisic acid, and *AhAPX88* under abscisic acid and paclobutrazol (**Figure 12B**). Notably, most of the genes did not show any expression under any type of stress conditions. The candidate genes with higher expression could be genetically engineered to improve the tolerance against multiple hormones and abiotic stress (cold and drought) conditions.

qRT-PCR-Based Expression Profiling of *AhAPX* Genes Under Cold and ABA Treatment

For qRT-PCR-based expression profiling, 10 highly upregulated *AhAPX* genes were selected based on transcriptome datasets to validate their transcript levels under ABA and cold treatment at various time points (**Figure 13**). Under ABA treatment, almost all genes demonstrated higher expression levels at all time points compared to CK, excluding a few cases. Such as, *AhAPX55* and *AhAPX140* showed relatively low expression at 9 and 12 h compared to CK and other time points (**Figure 13A**). In response to cold stress, although all the genes were upregulated; nevertheless, some genes showed relatively low expression levels compared to CK, such as *AhAPX4, AhAPX19, AhAPX55, AhAPX82, AhAPX102, AhAPX137,* and *AhAPX140*. Whereas *AhAPX17* and *AhAPX59* showed considerably higher expression than CK (**Figure 13B**). In short, all the preferred genes display parallel expression trends (i.e., upregulated) to those developed from transcriptome datasets (**Supplementary Figure 4**), therefore representing the reliability of the transcriptome datasets.

DISCUSSION

Characterization and Evolution of *APX* Gene Family in Plants

Cultivated peanut is widely known as an essential oilseed, protein-enrich food crop worldwide and retains important breeding traits during domestication (Zhuang et al., 2019; Bohra et al., 2022). Even so, peanut production is still substantially influenced by numerous biotic and abiotic factors (Agarwal et al., 2018; Gangurde et al., 2020, 2021; Kumar et al., 2020; Shasidhar et al., 2020; Sinha et al., 2020; Jadhav et al., 2021; Pandey et al., 2021; Soni et al., 2021; Aravind et al., 2022; Bomireddy et al., 2022; Liu et al., 2022; Patel et al., 2022). When plants are exposed to diverse abiotic and biotic factors,

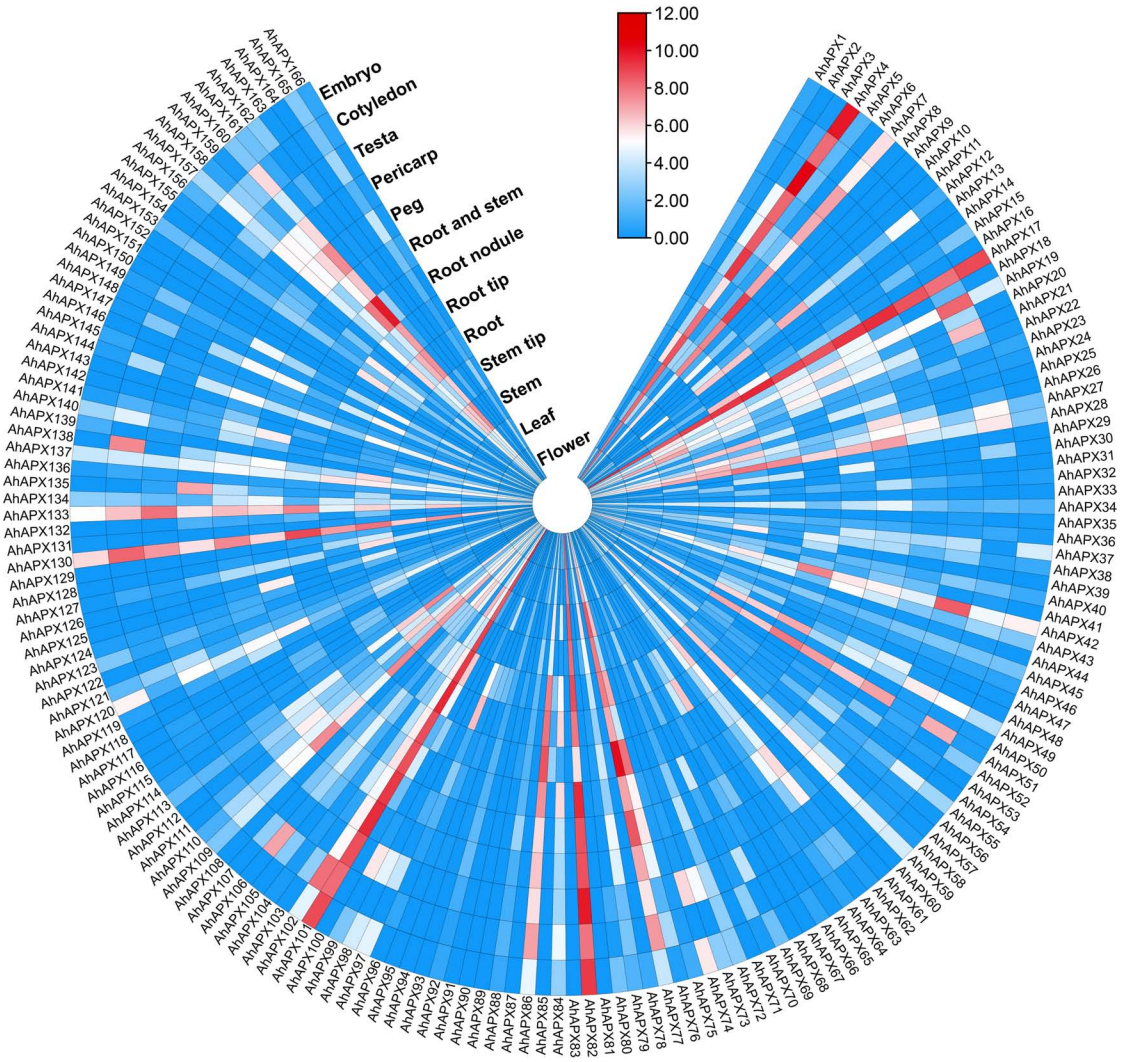

FIGURE 11 | Expression profiling of *AhAPX* genes in various developmental tissues of peanut. In the expression bar, the red, white and blue colors show high to low expression levels. The circular heat map was designed by taking log2 of fragments per kilobase of transcript per million (FPKM) values.

APX enzyme as a primary marker can quickly eliminate unnecessary H_2O_2 (i.e., ROS scavenging) from plant cells by adjusting several physiological and biochemical activities to safeguard cells from the noxiousness of overproduction of ROS (Das and Roychoudhury, 2014; Mittler, 2017; Hasanuzzaman et al., 2020, 2021). During the past few years, excessive advancement has been achieved in studying the mode of action of *APX* genes; however, their vital role still requires more examination. Recent peanut genome sequencing data allow us to comprehensively discover new gene family members and recognize their functional and defensive mechanisms against stress conditions.

Usually, *APX* gene family of plants comprises a few genes. In this study, 166 *AhAPX* genes have been discovered in peanut genome (**Supplementary Table 10**), a larger *APX* family than previously reported *APX* gene families in watermelon (Malambane et al., 2018), shrub (Wang et al., 2022), rice (Teixeira et al., 2004), *A. thaliana* (Panchuk et al., 2002, Panchuk et al., 2005), sorghum (Akbudak et al., 2018), kiwifruit (Liao et al., 2020), tomato (Najami et al., 2008), wheat (Tyagi et al., 2020), and cotton (Tao et al., 2018). Deviations in the *APX* members amongst diverse plant species may perhaps be attributed to gene duplication events involving tandem and segmental repeats and play a role in expanding *APXs* for deviation. Repetition of *APX* genes was also discovered in several plant species (Teixeira et al., 2004; Panchuk et al., 2005; Akbudak et al., 2018; Liao et al., 2020; Wang et al., 2022). Our outcomes confirmed that *AhAPXs* had suffered segmental duplications (**Supplementary Table 3**). Subsequently, these reports recommended that *AhAPXs* duplicate cases may possibly play an essential role in gene evolution.

Previous studies showed that *APX* family genes are usually clustered into four major groups based on their subcellular localization or tree topologies (Pandey et al., 2011;

Malambane et al., 2018; Tyagi et al., 2020). In the present study, all *APX* genes from four plant species were grouped into 11 main groups based on tree topologies and sequence similarities (**Figure 2**). This grouping was also recently supported by a new study on brassica crops (*B. napus* and *B. rapa*), where all *APX* genes were grouped into 13 subfamilies (Ma et al., 2021). Further, gene structure analysis also showed that genes belonging to the same subtree possess almost similar exon-intron patterns, ranging from 16 to 1 (exons) and 0 to 15 (introns) (**Figure 5B** and **Supplementary Table 10**). A significant difference was observed in gene structures where some genes have many exons-introns while some lack introns. Similar gene structure patterns were also reported in previous reports, such as in wheat number of exons extended from 7 to 12 (Tyagi et al., 2020). In *Actinidia chinensis*, the gene structure possesses 4–22 introns (Liao et al., 2020), which are higher than our observations. The exon-intron organization disparity was practiced by three important methods (exon/intron gain/loss, exonization/pseudoexonization, and insertion/deletion), and they are clearly supported by structural inconsistency (Xu et al., 2012). Notably, the *AhAPX* genes in each group almost exhibited comparable exon-intron group and conserved motifs (**Figure 5**), suggesting that these genes may possibly contribute to the similar tasks associated with several abiotic stressors. These outcomes are in agreement with earlier studies of kiwifruit (Liao et al., 2020), and wheat (Tyagi et al., 2020), where genes

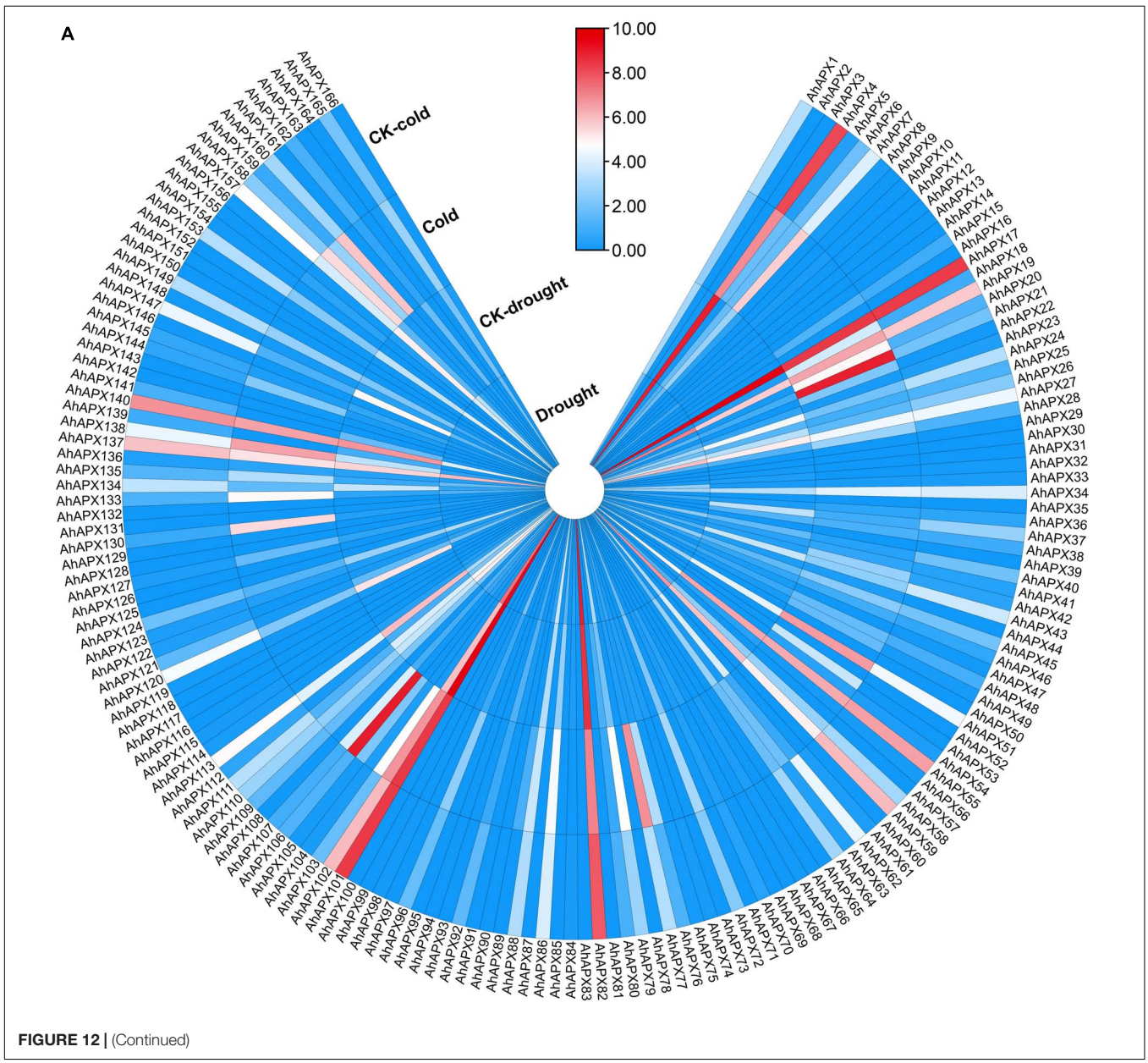

FIGURE 12 | (Continued)

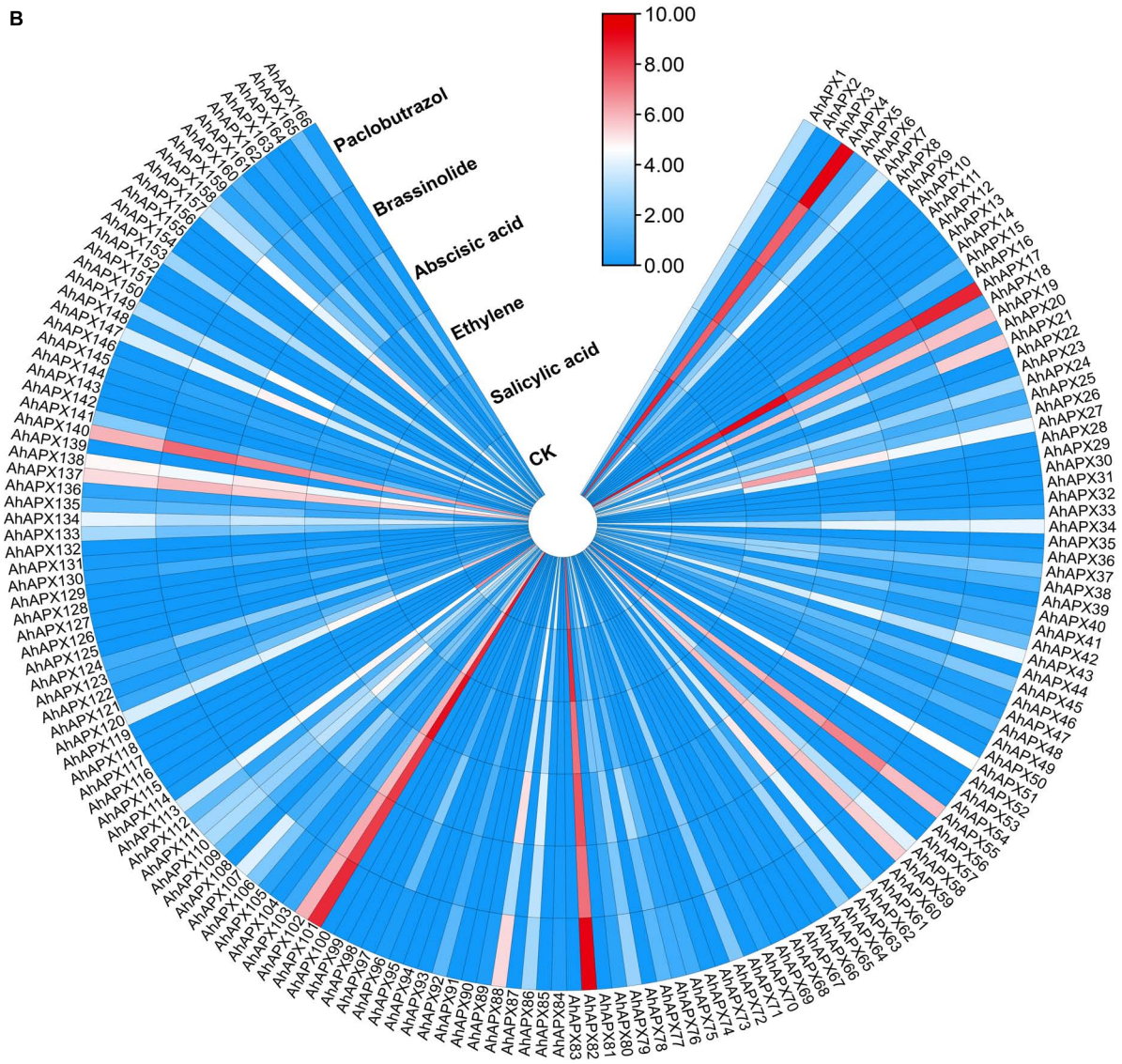

FIGURE 12 | Expression profiling of *AhAPX* genes under different **(A)** abiotic stress, including cold and drought stress, and **(B)** phytohormone treatments such as abscisic acid, salicylic acid, ethylene, brassinolide, and paclobutrazol. In both maps, the label "CK" refers to the control plants in comparison to the stress-treated plants. In the expression bar, the red, white and blue colors show high to low expression levels. The circular heat map was designed by taking log2 of fragments per kilobase of transcript per million (FPKM) values.

inside the same group comprise distinct structures and motifs organizations.

The Contribution of *APX* Genes Toward Stress Responses and Tolerance Mechanisms

To boost our understanding into the involvement of *AhAPX* genes contrary to numerous environmental factors, *cis*-elements were predicted in the promoter of *AhAPX* genes. The discoveries showed that three types of *cis*-elements were recognized, i.e., abiotic stress, phytohormones, and growth and development-related elements (**Figures 6**, **7**). Recent studies show that the *cis*-elements in *APX* genes contribute to the plant abiotic and phytohormones stress responses. Similar types of abiotic and phytohormone-related *cis*-regulatory elements have been identified in previous studies (Akbudak et al., 2018; Malambane et al., 2018; Tao et al., 2018; Liao et al., 2020; Tyagi et al., 2020; Wang et al., 2022). Furthermore, *AhAPXs* gene functions were further predicted by GO enrichment analysis (**Figure 10**), which also supported the role of these genes in ROS scavenging and stress response mechanisms. To get further insights into the role of *AhAPX* genes, their expression levels were examined under various hormones and abiotic stress treatments (**Figures 12**, **13**). Our results showed that a few genes significantly contribute to specific stress responses like

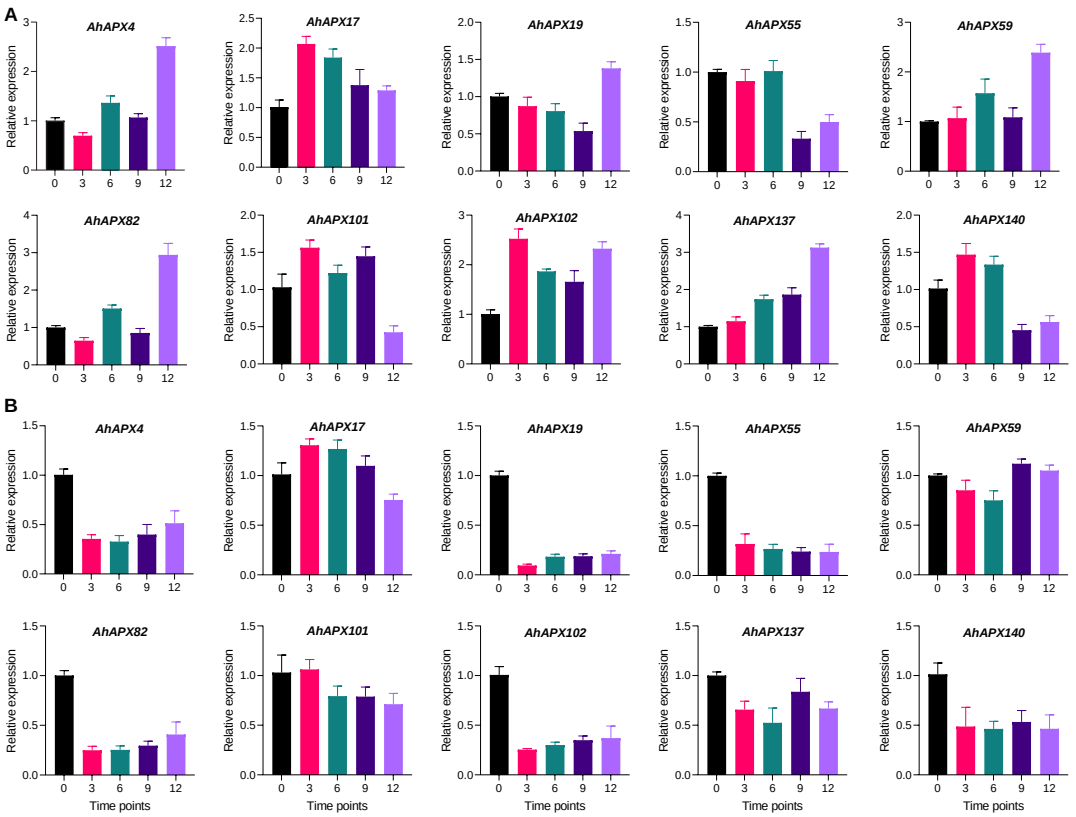

FIGURE 13 | Expression profiling of the *AhAPX* genes under **(A)** abscisic acid and **(B)** cold stress treatments. The time points include 0 (CK), 3, 6, 9, and 12 h when the samples were picked for expression analysis after the stress treatment. Error bars signify the SD of three biological repeats (n = 3).

cold, drought, and ABA. These results are in agreement with the previous reports of Akbudak et al. (2018), where some *SbAPX* genes were significantly induced by drought stress in the leaves and roots of two genotypes. Similarly, many genes showed higher expression levels in *A. nanus* under cold and osmotic stress (Wang et al., 2022). Many *BrAPX* and *BnAPX* genes showed higher expression trends in cold-tolerant varieties in response to cold stress (Ma et al., 2021). Under drought stress, most of the *ClAPX* genes were significantly upregulated and displayed elevated expression in watermelon (Malambane et al., 2018). These conclusions can enhance our perception of *AhAPX* genes under various stress conditions, especially cold and drought.

Recent reports also suggest that manipulating *APX* genes could contribute to stress tolerance in plants. For instance, a novel *ScAPX6* gene from sugarcane was overexpressed in tobacco (*Nicotiana benthamiana*), and transgenic plants showed improved resistance to the biotic stress (*Pseudomonas solanacearum* and *Fusarium solani*) by positively regulating the phytohormones contents (Liu et al., 2018). The overexpression of *PcAPX* from Chinese white poplar (*Populus tomentosa*) improves tolerance to multiple stresses, including salinity, drought, and oxidative stress in transgenic tobacco plants by improving biochemical mechanisms (Cao et al., 2017). Likewise, the overexpression of Populus peroxisomal *PpAPX* gene enhances drought stress tolerance in transgenic tobacco plants (Li et al., 2009). Transgenic tobacco overexpressing cytosolic *APX* gene alleviated the drought stress tolerance (Faize et al., 2011). Ectopic overexpression of the peroxisomal *SbpAPX* gene improves salinity tolerance in transgenic peanut (Singh et al., 2014). So far, this is the only *APX* gene that has been functionally characterized in peanut. These studies recommend that the genetic engineering of *APX* genes is of great importance in conferring various stress tolerance in crop plants, including peanut.

Among various identified TFs, ERF TFs have been functionally characterized from peanut. The results exhibited that overexpression of *AhERF008* impaired the root magnitude of *A. thaliana*; however, overexpression of *AhERF019* improved tolerance to heat, salinity and drought stresses in *A. thaliana* (Wan et al., 2014). Ectopic overexpression of MYB repressor gene (*GmMYB3a*) increases drought tolerance and physiological mechanisms in transgenic peanut under drought stress (He et al., 2020). Another NAC TF gene (*AhANC4*) from peanut enhances drought tolerance in transgenic tobacco plants due to improved stomatal closure and advanced water use efficiency (Tang et al., 2017). A novel WRKY TF gene (*AhWRKY75*) improved salinity tolerance in transgenic peanut plants by improving antioxidant mechanisms, ROS scavenging, stomatal conductance, and

photosynthesis under salinity stress (Zhu et al., 2021). All these studies suggest that the genetic engineering of TF is a promising approach to improve peanut performance under stressed conditions.

The Contribution of *APX* Genes in Numerous Organs/Tissues

Here, the tissue-specific expression profiling of 166 *AhAPX* genes was carried out in various organs/tissues using publically available transcriptome datasets. Overall, the results showed that only a few *AhAPX* genes showed higher expression levels, particularly in roots, stem, leaf, peg, pericarp, testa, and flowers (**Figure 11**). In *A. nanus*, the RNA-seq data was used to observe the expression levels in leaves. The results displayed that only one gene showed substantially higher expression in leaf (Wang et al., 2022). In wheat, most of the genes showed higher expression patterns in root, stem, leaf, spike, and grain. Especially, almost half of the *APX* genes were found to be leaf-specific due to significantly higher expression (Tyagi et al., 2020). In *A. chinensis*, qRT-PCR-based expression profiling of 13 *AhAPX* genes was performed in various fruit developmental stages. The outcomes demonstrated that eight *AcAPX* genes had the utmost expression patterns during the color turn-off phase (Liao et al., 2020). It can be concluded that the tissue-specific *APX* genes (such as *AhAPX4, AhAPX17, AhAPX77, AhAPX82, AhAPX101,* and *AhAPX130*) could be considered as target candidates for further molecular studies to fully reveal their role and mechanisms in peanut growth and development.

MicroRNA: Emerging Players for Crop Improvement and Stress Tolerance

MicroRNAs (miRNAs) are a group of tiny-non-coding RNAs formed from individual-strand hairpin RNA precursors. These miRNAs switch gene expression by attaching to corresponding sequences surrounded by target mRNAs (Jamla et al., 2021; Patil et al., 2021). Extensive progress has been put together in finding the targets of peanut miRNAs that contribute to various stresses and developmental activities (Zhao et al., 2010, 2015; Chi et al., 2011; Zhang et al., 2017; Chen H. et al., 2019; Figueredo et al., 2020; Tong et al., 2021). The present predicted 14 miRNAs belonging to 12 different families targeting 33 *AhAPX* genes (**Figure 8** and **Supplementary Table 6**). Notably, none of the previous studies predicted the miRNAs that can target *APX* genes, expect one study. A recent study supports our findings where 51 miRNAs have been identified targeting 29 *TaAPX* genes in wheat (Tyagi et al., 2020). However, these target genes are yet to be characterized in wheat. In another study, a new miRNA (ath-miR447a-3p) was found to be targeting *APX3* gene, and its expression analysis showed that it negatively regulated the expression of *APX3,* which is directly involved in the APX synthesis under drought stress in *Zanthoxylum bungeanum* (Fei et al., 2020).

However, some of the identified miRNAs have been reported to take part in stress tolerance and developmental processes. For instance, spatio-temporal expression patterns of miRNA159 family representatives have been found targeting *MYB* genes in grapevine (*Vitis vinifera* L.). The results showed that *miRNA159c-VvGAMYB* module is involved in gibberellin-tempted parthenocarpy in grapevine (Wang et al., 2018). Another study discovered that miR167A is the main member of miR167 family that regulates the *A. thaliana* reproduction. Further, miR167A acts as a parental gene that works mostly *via ARF6* and *ARF8* genes in maternal management of embryonic and seed growth (Yao et al., 2019). A member of miRNA156 family has been reported to be involved in the interaction between ABA and miRNA156, which regulates the expression profile of anthocyanin biogenesis genes in drought-stressed plants (González-Villagra et al., 2017). Notably, several miRNA families such as miR3513, miR3518, miR3520, miR3513, miR3516, etc., have not been functionally characterized; therefore, the future work could also be focused on these unique miRNAs to reveal their potential in plant growth and development. Moreover, the expression profiling of prophesied miRNAs and their targeted genes demands validation to direct their biological roles in the peanut breeding programs.

CONCLUSION

Altogether, we recognized 166 putative *AhAPX* genes in the cultivated peanut genome, which are mapped on all chromosomes, including unassembled ones. Comprehensive *in silico* examination of *AhAPX* genes, i.e., characterization, evolution, gene structure, conserved motifs, *cis*-elements, putative miRNA and TFs prediction, GO and KEGG enrichment were executed to increase our understanding of *AhAPX* genes in peanut. Their expression trends were also evaluated in various developmental organs/tissues, phytohormones, and abiotic stress conditions. In brief, this report set the foundation for further functional experiments (such as overexpression, gene editing *via* CRISPR/Cas system, etc.) of some candidate genes such as *AhAPX4/17/19/55/59/82/101/102/137* and *AhAPX140*, which can advance the peanut breeding programs under undesirable stress conditions.

DATA AVAILABILITY STATEMENT

The datasets presented in this study can be found in online repositories. The names of the repository/repositories and accession number(s) can be found below: NCBI BioProject–PRJNA480120.

AUTHOR CONTRIBUTIONS

AR and WZ conceived the idea. AR analyzed the data and wrote the manuscript. YS and KC helped with qRT-PCR

analysis. YS, KC, CZ, LW, HF, AC, and HC helped in literature search and data analysis. WZ and RKV supervised the research, and reviewed and improved the manuscript. All authors have read and approved the final version of the manuscript.

FUNDING

This work was supported by grants from the National Science Foundation (NSF) of China (U1705233, 32072103, and 31701463), the Science and Technology Foundation of Fujian Province of China (2021N5007), and Fujian Agriculture and Forestry University, Fuzhou, China. RKV is thankful to Food Futures Institute, Murdoch University, Australia, for supporting this study in part.

ACKNOWLEDGMENTS

RKV is thankful to Food Futures Institute, Murdoch University, Australia, for supporting this study in part.

SUPPLEMENTARY MATERIAL

The Supplementary Material for this article can be found online at: https://www.frontiersin.org/articles/10.3389/fpls.2022.962182/full#supplementary-material

REFERENCES

Agarwal, G., Clevenger, J., Pandey, M. K., Wang, H., Shasidhar, Y., Chu, Y., et al. (2018). High-density genetic map using whole-genome resequencing for fine mapping and candidate gene discovery for disease resistance in peanut. *Plant Biotechnol. J.* 16, 1954–1967. doi: 10.1111/pbi.12930

Akbudak, M. A., Filiz, E., Vatansever, R., and Kontbay, K. (2018). Genome-wide identification and expression profiling of ascorbate peroxidase (APX) and glutathione peroxidase (GPX) genes under drought stress in sorghum (*Sorghum bicolor* L.). *J. Plant Growth Regulat.* 37, 925–936.

Aravind, B., Nayak, S. N., Choudhary, R. S., Gandhadmath, S. S., Prasad, P., Pandey, M. K., et al. (2022). "Integration of genomics approaches in abiotic stress tolerance in groundnut (L.): an overview," in *Genomic Designing for Abiotic Stress Resistant Oilseed Crops*, ed. C. Kole (Cham: Springer), 149–197.

Bailey, T. L., Boden, M., Buske, F. A., Frith, M., Grant, C. E., Clementi, L., et al. (2009). MEME SUITE: tools for motif discovery and searching. *Nucleic Acids Res.* 37(Suppl._2), W202–W208.

Bertioli, D. J., Jenkins, J., Clevenger, J., Dudchenko, O., Gao, D., Seijo, G., et al. (2019). The genome sequence of segmental allotetraploid peanut *Arachis hypogaea*. *Nat. Genet.* 51, 877–884. doi: 10.1038/s41588-019-0405-z

Bohra, A., Tiwari, A., Kaur, P., Ganie, S. A., Raza, A., Roorkiwal, M., et al. (2022). The key to the future lies in the past: insights from grain legume domestication and improvement should inform future breeding strategies. *Plant Cell Physiol.* [Online ahead of print]. doi: 10.1093/pcp/pcac086

Bomireddy, D., Gangurde, S. S., Variath, M. T., Janila, P., Manohar, S. S., Sharma, V., et al. (2022). Discovery of major quantitative trait loci and candidate genes for fresh seed dormancy in groundnut. *Agronomy* 12:404.

Cannon, S. B., Mitra, A., Baumgarten, A., Young, N. D., and May, G. (2004). The roles of segmental and tandem gene duplication in the evolution of large gene families in *Arabidopsis thaliana*. *BMC Plant Biol.* 4:10. doi: 10.1186/1471-2229-4-10

Cao, S., Du, X.-H., Li, L.-H., Liu, Y.-D., Zhang, L., Pan, X., et al. (2017). Overexpression of *Populus tomentosa* cytosolic ascorbate peroxidase enhances abiotic stress tolerance in tobacco plants. *Russ. J. Plant Physiol.* 64, 224–234.

Chen, C., Chen, H., Zhang, Y., Thomas, H. R., Frank, M. H., He, Y., et al. (2020). TBtools: an integrative toolkit developed for interactive analyses of big biological data. *Mol. Plant* 13, 1194–1202. doi: 10.1016/j.molp.2020.06.009

Chen, H., Yang, Q., Chen, K., Zhao, S., Zhang, C., Pan, R., et al. (2019). Integrated microRNA and transcriptome profiling reveals a miRNA-mediated regulatory network of embryo abortion under calcium deficiency in peanut (*Arachis hypogaea* L.). *BMC Genomics* 20:392. doi: 10.1186/s12864-019-5770-6

Chen, X., Lu, Q., Liu, H., Zhang, J., Hong, Y., Lan, H., et al. (2019). Sequencing of cultivated peanut, *Arachis hypogaea*, yields insights into genome evolution and oil improvement. *Mol. Plant* 12, 920–934. doi: 10.1016/j.molp.2019.03.005

Chi, X., Hu, R., Yang, Q., Zhang, X., Pan, L., Chen, N., et al. (2012). Validation of reference genes for gene expression studies in peanut by quantitative real-time RT-PCR. *Mol. Genet. Genomics* 287, 167–176.

Chi, X., Yang, Q., Chen, X., Wang, J., Pan, L., Chen, M., et al. (2011). Identification and characterization of microRNAs from peanut (*Arachis hypogaea* L.) by high-throughput sequencing. *PLoS One* 6:e27530. doi: 10.1371/journal.pone.0027530

Dai, X., Zhuang, Z., and Zhao, P. X. (2018). psRNATarget: a plant small RNA target analysis server (2017 release). *Nucleic Acids Res.* 46, W49–W54. doi: 10.1093/nar/gky316

Das, K., and Roychoudhury, A. (2014). Reactive oxygen species (ROS) and response of antioxidants as ROS-scavengers during environmental stress in plants. *Front. Environ. Sci.* 2:53. doi: 10.3389/fenvs.2014.00053

Dash, S., Cannon, E. K., Kalberer, S. R., Farmer, A. D., and Cannon, S. B. (2016). "PeanutBase and other bioinformatic resources for peanut," in *Peanuts: Genetics, Processing, and Utilization*, ed. H. Thomas (Amsterdam: Elsevier), 241–252.

El-Gebali, S., Mistry, J., Bateman, A., Eddy, S. R., Luciani, A., Potter, S. C., et al. (2019). The Pfam protein families database in 2019. *Nucleic Acids Res.* 47, D427–D432.

Fahad, S., Bajwa, A. A., Nazir, U., Anjum, S. A., Farooq, A., Zohaib, A., et al. (2017). Crop production under drought and heat stress: plant responses and management options. *Front. Plant Sci.* 8:1147. doi: 10.3389/fpls.2017.01147

Fahad, S., Nie, L., Chen, Y., Wu, C., Xiong, D., Saud, S., et al. (2015). "Crop plant hormones and environmental stress," in *Sustainable Agriculture Reviews. Sustainable Agriculture Reviews*, Vol. 15, ed. E. Lichtfouse (Cham: Springer), 371–400.

Faize, M., Burgos, L., Faize, L., Piqueras, A., Nicolas, E., Barba-Espin, G., et al. (2011). Involvement of cytosolic ascorbate peroxidase and Cu/Zn-superoxide dismutase for improved tolerance against drought stress. *J. Exp. Bot.* 62, 2599–2613.

Fei, X., Li, J., Kong, L., Hu, H., Tian, J., Liu, Y., et al. (2020). miRNAs and their target genes regulate the antioxidant system of *Zanthoxylum bungeanum* under drought stress. *Plant Physiol. Biochem.* 150, 196–203.

Figueredo, M. S., Formey, D., Rodríguez, J., Ibáñez, F., Hernández, G., and Fabra, A. (2020). Identification of miRNAs linked to peanut nodule functional processes. *J. Biosci.* 45, 1–7.

Finn, R. D., Clements, J., Arndt, W., Miller, B. L., Wheeler, T. J., Schreiber, F., et al. (2015). HMMER web server: 2015 update. *Nucleic Acids Res.* 43, W30–W38. doi: 10.1093/nar/gkv397

Gangurde, S. S., Nayak, S. N., Joshi, P., Purohit, S., Sudini, H. K., Chitikineni, A., et al. (2021). Comparative transcriptome analysis identified candidate genes for late leaf spot resistance and cause of defoliation in groundnut. *Int. J. Mol. Sci.* 22:4491. doi: 10.3390/ijms22094491

Gangurde, S. S., Wang, H., Yaduru, S., Pandey, M. K., Fountain, J. C., Chu, Y., et al. (2020). Nested-association mapping (NAM)-based genetic dissection uncovers candidate genes for seed and pod weights in peanut (*Arachis hypogaea*). *Plant Biotechnol. J.* 18, 1457–1471. doi: 10.1111/pbi.13311

Gasteiger, E., Hoogland, C., Gattiker, A., Wilkins, M. R., Appel, R. D., and Bairoch, A. (2005). "Protein identification and analysis tools on the ExPASy server," in

The Proteomics Protocols Handbook, ed. J. M. Walker (Totowa, NJ: Humana Press), 571–607.

González-Villagra, J., Kurepin, L. V., and Reyes-Díaz, M. M. (2017). Evaluating the involvement and interaction of abscisic acid and miRNA156 in the induction of anthocyanin biosynthesis in drought-stressed plants. *Planta* 246, 299–312.

Hasanuzzaman, M., Bhuyan, M., Zulfiqar, F., Raza, A., Mohsin, S. M., Mahmud, J. A., et al. (2020). Reactive oxygen species and antioxidant defense in plants under abiotic stress: revisiting the crucial role of a universal defense regulator. *Antioxidants* 9:681. doi: 10.3390/antiox9080681

Hasanuzzaman, M., Raihan, M., Hossain, R., Masud, A. A. C., Rahman, K., Nowroz, F., et al. (2021). Regulation of reactive oxygen species and antioxidant defense in plants under salinity. *Int. J. Mol. Sci.* 22:9326.

He, Y., Mu, S., He, Z., Wang, B., and Li, Y. (2020). Ectopic expression of MYB repressor GmMYB3a improves drought tolerance and productivity of transgenic peanuts (*Arachis hypogaea* L.) under conditions of water deficit. *Transgen. Res.* 29, 563–574. doi: 10.1007/s11248-020-00220-z

Hodges, D. M., DeLong, J. M., Forney, C. F., and Prange, R. K. (1999). Improving the thiobarbituric acid-reactive-substances assay for estimating lipid peroxidation in plant tissues containing anthocyanin and other interfering compounds. *Planta* 207, 604–611. doi: 10.1007/s00425-017-2699-3

Hurst, L. D. (2002). The Ka/Ks ratio: diagnosing the form of sequence evolution. *Trend. Genet.* 18, 486–486. doi: 10.1016/s0168-9525(02)02722-1

Jadhav, M. P., Gangurde, S. S., Hake, A. A., Yadawad, A., Mahadevaiah, S. S., Pattanashetti, S. K., et al. (2021). Genotyping-by-sequencing based genetic mapping identified major and consistent genomic regions for productivity and quality traits in peanut. *Front. Plant Sci.* 12:668020. doi: 10.3389/fpls.2021.668020

Jamla, M., Patil, S., Joshi, S., Khare, T., and Kumar, V. (2021). MicroRNAs and their exploration for developing heavy metal-tolerant plants. *J Plant Growth Regulat.* 9, 1–17.

Kumar, R., Janila, P., Vishwakarma, M. K., Khan, A. W., Manohar, S. S., Gangurde, S. S., et al. (2020). Whole-genome resequencing-based QTL-seq identified candidate genes and molecular markers for fresh seed dormancy in groundnut. *Plant Biotechnol. J.* 18, 992–1003. doi: 10.1111/pbi.13266

Kumar, S., Stecher, G., Li, M., Knyaz, C., and Tamura, K. (2018). MEGA X: molecular evolutionary genetics analysis across computing platforms. *Mol. Biol. Evol.* 35, 1547–1549. doi: 10.1093/molbev/msy096

Lazzarotto, F., Teixeira, F. K., Rosa, S. B., Dunand, C., Fernandes, C. L., de Vasconcelos Fontenele, A., et al. (2011). Ascorbate peroxidase-related (APx-R) is a new heme-containing protein functionally associated with ascorbate peroxidase but evolutionarily divergent. *New Phytol.* 191, 234–250. doi: 10.1111/j.1469-8137.2011.03659.x

Lescot, M., Déhais, P., Thijs, G., Marchal, K., Moreau, Y., Van de Peer, Y., et al. (2002). PlantCARE, a database of plant cis-acting regulatory elements and a portal to tools for in silico analysis of promoter sequences. *Nucleic Acids Res.* 30, 325–327. doi: 10.1093/nar/30.1.325

Letunic, I., and Bork, P. (2021). Interactive Tree Of Life (iTOL) v5: an online tool for phylogenetic tree display and annotation. *Nucleic Acids Res.* 49, W293–W296. doi: 10.1093/nar/gkab301

Li, W., Huai, X., Li, P., Raza, A., Mubarik, M. S., Habib, M., et al. (2021). Genome-wide characterization of glutathione peroxidase (GPX) gene family in rapeseed (*Brassica napus* L.) revealed their role in multiple abiotic stress response and hormone signaling. *Antioxidants* 10:1481. doi: 10.3390/antiox10091481

Li, Y. J., Hai, R. L., Du, X. H., Jiang, X. N., and Lu, H. (2009). Over-expression of a Populus peroxisomal ascorbate peroxidase (PpAPX) gene in tobacco plants enhances stress tolerance. *Plant Breed.* 128, 404–410.

Liao, G.-L., Liu, Q., Li, Y.-Q., Zhong, M., Huang, C.-H., Jia, D.-F., et al. (2020). Identification and expression profiling analysis of ascorbate peroxidase gene family in *Actinidia chinensis* (Hongyang). *J. Plant Res.* 133, 715–726. doi: 10.1007/s10265-020-01206-y

Liu, F., Huang, N., Wang, L., Ling, H., Sun, T., Ahmad, W., et al. (2018). A novel L-ascorbate peroxidase 6 gene, ScAPX6, plays an important role in the regulation of response to biotic and abiotic stresses in sugarcane. *Front. Plant Sci.* 8:2262. doi: 10.3389/fpls.2017.02262

Liu, Y., Shao, L., Zhou, J., Li, R., Pandey, M. K., Han, Y., et al. (2022). Genomic insights into the genetic signatures of selection and seed trait loci in cultivated peanut. *J. Adv. Res.* doi: 10.1016/j.jare.2022.01.016

Livak, K. J., and Schmittgen, T. D. (2001). Analysis of relative gene expression data using real-time quantitative PCR and the 2- ΔΔCT method. *Methods* 25, 402–408.

Ma, L., Bai, J., Xu, J., Qi, W., Li, H., Fang, Y., et al. (2021). *Identification of Proteins Involved in Response to Cold Stress and Genome-Wide Identification and Analysis of the APX Gene Family in Winter Rapeseed (Brassica rapa L.)*. Available online at: https://www.researchsquare.com/article/rs-538668/v1.pdf (accessed June 7, 2021)

Malambane, G., Tsujimoto, H., and Akashi, K. (2018). The cDNA structures and expression profile of the ascorbate peroxidase gene family during drought stress in wild watermelon. *J. Agric. Sci.* 10, 56–71.

Mir, R. A., Bhat, B. A., Yousuf, H., Islam, S. T., Raza, A., Rizvi, M. A., et al. (2022). Multidimensional role of silicon to activate resilient plant growth and to mitigate abiotic stress. *Front. Plant Sci.* 13:819658. doi: 10.3389/fpls.2022.819658

Mittler, R. (2017). ROS are good. *Trends Plant Sci.* 22, 11–19.

Najami, N., Janda, T., Barriah, W., Kayam, G., Tal, M., Guy, M., et al. (2008). Ascorbate peroxidase gene family in tomato: its identification and characterization. *Mol. Genet. Genomics* 279, 171–182. doi: 10.1007/s00438-007-0305-2

Panchuk, I. I, Volkov, R. A., and Schoffl, F. (2002). Heat stress-and heat shock transcription factor-dependent expression and activity of ascorbate peroxidase in Arabidopsis. *Plant Physiol.* 129, 838–853. doi: 10.1104/pp.001362

Panchuk, I. I., Zentgraf, U., and Volkov, R. A. (2005). Expression of the Apx gene family during leaf senescence of *Arabidopsis thaliana*. *Planta* 222, 926–932. doi: 10.1007/s00425-005-0028-8

Pandey, M., Gangurde, S., Sharma, V., Pattanashetti, S., Naidu, G., Faye, I., et al. (2021). Improved genetic map identified major qtls for drought tolerance-and iron deficiency tolerance-related traits in groundnut. *Genes* 30:37. doi: 10.3390/genes12010037

Pandey, M. K., Gangurde, S. S., Sharma, V., Pattanashetti, S. K., Naidu, G. K., Faye, I., et al. (2020). Improved genetic map identified major QTLs for drought tolerance-and iron deficiency tolerance-related traits in groundnut. *Genes* 12:37.

Pandey, S., Fartyal, D., Agarwal, A., Shukla, T., James, D., Kaul, T., et al. (2017). Abiotic stress tolerance in plants: myriad roles of ascorbate peroxidase. *Front. Plant Sci.* 8:581. doi: 10.3389/fpls.2017.00581

Pandey, S., Negi, Y., Marla, S., and Arora, S. (2011). Comparative in silico analysis of ascorbate peroxidase protein sequences from different plant species. *J. Bioeng. Biomed. Sci.* 1:2. doi: 10.4238/2013.February.27.3

Patel, J., Khandwal, D., Choudhary, B., Ardeshana, D., Jha, R. K., Tanna, B., et al. (2022). Differential physio-biochemical and metabolic responses of peanut (*Arachis hypogaea* L.) under multiple abiotic stress conditions. *Int. J. Mol. Sci.* 23:660. doi: 10.3390/ijms23020660

Patil, S., Joshi, S., Jamla, M., Zhou, X., Taherzadeh, M. J., Suprasanna, P., et al. (2021). MicroRNA-mediated bioengineering for climate-resilience in crops. *Bioengineered* 12, 10430–10456. doi: 10.1080/21655979.2021.1997244

Powell, S., Forslund, K., Szklarczyk, D., Trachana, K., Roth, A., Huerta-Cepas, J., et al. (2014). eggNOG v4. 0: nested orthology inference across 3686 organisms. *Nucleic Acids Res.* 42, D231–D239. doi: 10.1093/nar/gkt1253

Raza, A., Hussain, S., Javed, R., Hafeez, M. B., and Hasanuzzaman, M. (2021a). "Antioxidant defense systems and remediation of metal toxicity in plants," in *Approaches to the Remediation of Inorganic Pollutants*, ed. M. Hasanuzzaman (Singapore: Springer), 91–124.

Raza, A., Su, W., Gao, A., Mehmood, S. S., Hussain, M. A., Nie, W., et al. (2021b). Catalase (CAT) gene family in rapeseed (*Brassica napus* L.): genome-wide analysis, identification, and expression pattern in response to multiple hormones and abiotic stress conditions. *Int. J. Mol. Sci.* 22:4281. doi: 10.3390/ijms22084281

Raza, A., Tabassum, J., Mubarik, M., Anwar, S., Zahra, N., Sharif, Y., et al. (2022a). Hydrogen sulfide: an emerging component against abiotic stress in plants. *Plant Biol.* 24, 540–558.

Raza, A., Tabassum, J., Zahid, Z., Charagh, S., Bashir, S., Barmukh, R., et al. (2022b). Advances in "Omics" approaches for improving toxic metals/metalloids tolerance in plants. *Front. Plant Sci.* 12:794373. doi: 10.3389/fpls.2021.794373

Rhee, S. Y., Beavis, W., Berardini, T. Z., Chen, G., Dixon, D., Doyle, A., et al. (2003). The Arabidopsis Information Resource (TAIR): a model organism database

providing a centralized, curated gateway to Arabidopsis biology, research materials and community. *Nucleic Acids Res.* 31, 224–228. doi: 10.1093/nar/gkg076

Sabagh, A. E., Mbarki, S., Hossain, A., Iqbal, M., Islam, M., Raza, A., et al. (2021). Potential role of plant growth regulators in administering crucial processes against abiotic stresses. *Front. Agron.* 3:648694. doi: 10.3389/fagro.2021.648694

Saeed, F., Chaudhry, U. K., Bakhsh, A., Raza, A., Saeed, Y., Bohra, A., et al. (2022). Moving beyond DNA sequence to improve plant stress responses. *Front. Genet.* 13:874648. doi: 10.3389/fgene.2022.874648

Shannon, P., Markiel, A., Ozier, O., Baliga, N. S., Wang, J. T., Ramage, D., et al. (2003). Cytoscape: a software environment for integrated models of biomolecular interaction networks. *Genome Res.* 13, 2498–2504. doi: 10.1101/gr.1239303

Sharif, Y., Chen, H., Deng, Y., Ali, N., Khan, S. A., Zhang, C., et al. (2021). Cloning and functional characterization of a pericarp abundant expression promoter (*AhGLP17-1P*) from peanut (*Arachis hypogaea* L.). *Front. Genet.* 12:821281. doi: 10.3389/fgene.2021.821281

Sharma, M., Kumar, P., Verma, V., Sharma, R., Bhargava, B., and Irfan, M. (2022). Understanding plant stress memory response for abiotic stress resilience: molecular insights and prospects. *Plant Physiol. Biochem.* 179, 10–24. doi: 10.1016/j.plaphy.2022.03.004

Shasidhar, Y., Variath, M. T., Vishwakarma, M. K., Manohar, S. S., Gangurde, S. S., Sriswathi, M., et al. (2020). Improvement of three popular Indian groundnut varieties for foliar disease resistance and high oleic acid using SSR markers and SNP array in marker-assisted backcrossing. *Crop J.* 8, 1–15.

Singh, N., Mishra, A., and Jha, B. (2014). Ectopic over-expression of peroxisomal ascorbate peroxidase (SbpAPX) gene confers salt stress tolerance in transgenic peanut (*Arachis hypogaea*). *Gene* 547, 119–125. doi: 10.1016/j.gene.2014.06.037

Sinha, P., Bajaj, P., Pazhamala, L. T., Nayak, S. N., Pandey, M. K., Chitikineni, A., et al. (2020). *Arachis hypogaea* gene expression atlas for fastigiata subspecies of cultivated groundnut to accelerate functional and translational genomics applications. *Plant Biotechnol. J.* 18, 2187–2200. doi: 10.1111/pbi.13374

Soni, P., Pandey, A. K., Nayak, S. N., Pandey, M. K., Tolani, P., Pandey, S., et al. (2021). Global transcriptome profiling identified transcription factors, biological process, and associated pathways for pre-harvest aflatoxin contamination in groundnut. *J. Fungi* 7:413. doi: 10.3390/jof7060413

Su, W., Raza, A., Gao, A., Jia, Z., Zhang, Y., Hussain, M. A., et al. (2021). Genome-wide analysis and expression profile of superoxide dismutase (SOD) gene family in rapeseed (*Brassica napus* L.) under different hormones and abiotic stress conditions. *Antioxidants* 10:1182. doi: 10.3390/antiox10081182

Swift, M. L. (1997). GraphPad prism, data analysis, and scientific graphing. *J. Chem. Informat. Comput. Sci.* 37, 411–412.

Tang, G., Shao, F., Xu, P., Shan, L., and Liu, Z. (2017). Overexpression of a peanut NAC gene, AhNAC4, confers enhanced drought tolerance in tobacco. *Russ. J. Plant Physiol.* 64, 525–535. doi: 10.3389/fpls.2022.817106

Tao, C., Jin, X., Zhu, L., Xie, Q., Wang, X., and Li, H. (2018). Genome-wide investigation and expression profiling of APX gene family in *Gossypium hirsutum* provide new insights in redox homeostasis maintenance during different fiber development stages. *Mol. Genet. Genomics* 293, 685–697. doi: 10.1007/s00438-017-1413-2

Teixeira, F. K., Menezes-Benavente, L., Margis, R., and Margis-Pinheiro, M. (2004). Analysis of the molecular evolutionary history of the ascorbate peroxidase gene family: inferences from the rice genome. *J. Mol. Evol.* 59, 761–770. doi: 10.1007/s00239-004-2666-z

Tian, F., Yang, D.-C., Meng, Y.-Q., Jin, J., and Gao, G. (2020). PlantRegMap: charting functional regulatory maps in plants. *Nucleic Acids Res.* 48, D1104–D1113. doi: 10.1093/nar/gkz1020

Tong, B., Shi, Y., Ntambiyukuri, A., Li, X., Zhan, J., Wang, A., et al. (2021). Integration of Small RNA and degradome sequencing reveals the regulatory network of al-induced programmed cell death in peanut. *Int. J. Mol. Sci.* 23:246. doi: 10.3390/ijms23010246

Tyagi, S., Verma, P. C., Singh, K., and Upadhyay, S. K. (2020). Molecular characterization of ascorbate peroxidase (APX) and APX-related (APX-R) genes in *Triticum aestivum* L. *Genomics* 112, 4208–4223. doi: 10.1016/j.ygeno.2020.07.023

Varshney, R. K., Bohra, A., Roorkiwal, M., Barmukh, R., Cowling, W. A., Chitikineni, A., et al. (2021a). Fast-forward breeding for a food-secure world. *Trends Genet.* 37, 1124–1136. doi: 10.1016/j.tig.2021.08.002

Varshney, R. K., Bohra, A., Yu, J., Graner, A., Zhang, Q., and Sorrells, M. E. (2021b). Designing future crops: genomics-assisted breeding comes of age. *Trends Plant Sci.* 26, 631–649. doi: 10.1016/j.tplants.2021.03.010

Varshney, R. K., Pandey, M. K., Bohra, A., Singh, V. K., Thudi, M., and Saxena, R. K. (2019). Toward the sequence-based breeding in legumes in the post-genome sequencing era. *Theor. Appl. Genet.* 132, 797–816. doi: 10.1007/s00122-018-3252-x

Varshney, R. K., Sinha, P., Singh, V. K., Kumar, A., Zhang, Q., and Bennetzen, J. L. (2020). 5Gs for crop genetic improvement. *Curr. Opin. Plant Biol.* 56, 190–196. doi: 10.1016/j.pbi.2019.12.004

Wan, L., Wu, Y., Huang, J., Dai, X., Lei, Y., Yan, L., et al. (2014). Identification of ERF genes in peanuts and functional analysis of AhERF008 and AhERF019 in abiotic stress response. *Funct. Integr. Genomics* 14, 467–477. doi: 10.1007/s10142-014-0381-4

Wang, C., Jogaiah, S., Zhang, W., Abdelrahman, M., and Fang, J. G. (2018). Spatio-temporal expression of miRNA159 family members and their GAMYB target gene during the modulation of gibberellin-induced grapevine parthenocarpy. *J. Exp. Bot.* 69, 3639–3650. doi: 10.1093/jxb/ery172

Wang, Y., Cao, S., Sui, X., Wang, J., Geng, Y., Gao, F., et al. (2022). Genome-wide characterization, evolution, and expression analysis of the ascorbate peroxidase and glutathione peroxidase gene families in response to cold and osmotic stress in *Ammopiptanthus nanus*. *J. Plant Growth Regul.* 1–21. doi: 10.1007/s00344-021-10570-5

Xu, G., Guo, C., Shan, H., and Kong, H. (2012). Divergence of duplicate genes in exon–intron structure. *Proc. Natl. Acad. Sci.* 109, 1187–1192.

Yao, X., Chen, J., Zhou, J., Yu, H., Ge, C., Zhang, M., et al. (2019). An essential role for miRNA167 in maternal control of embryonic and seed development. *Plant Physiol.* 180, 453–464. doi: 10.1104/pp.19.00127

Yu, C. S., Chen, Y. C., Lu, C. H., and Hwang, J. K. (2006). Prediction of protein subcellular localization. *Proteins* 64, 643–651.

Zhang, T., Hu, S., Yan, C., Li, C., Zhao, X., Wan, S., et al. (2017). Mining, identification and function analysis of microRNAs and target genes in peanut (*Arachis hypogaea* L.). *Plant Physiol. Biochem.* 111, 85–96. doi: 10.1016/j.plaphy.2016.11.018

Zhao, C., Xia, H., Cao, T., Yang, Y., Zhao, S., Hou, L., et al. (2015). Small RNA and degradome deep sequencing reveals peanut microRNA roles in response to pathogen infection. *Plant Mol. Biol. Rep.* 33, 1013–1029.

Zhao, C.-Z., Xia, H., Frazier, T. P., Yao, Y.-Y., Bi, Y.-P., Li, A.-Q., et al. (2010). Deep sequencing identifies novel and conserved microRNAs in peanuts (*Arachis hypogaea* L.). *BMC Plant Biol.* 10:3. doi: 10.1186/1471-2229-10-3

Zhu, H., Jiang, Y., Guo, Y., Huang, J., Zhou, M., Tang, Y., et al. (2021). A novel salt inducible WRKY transcription factor gene, AhWRKY75, confers salt tolerance in transgenic peanut. *Plant Physiol. Biochem.* 160, 175–183. doi: 10.1016/j.plaphy.2021.01.014

Zhuang, W., Chen, H., Yang, M., Wang, J., Pandey, M. K., Zhang, C., et al. (2019). The genome of cultivated peanut provides insight into legume karyotypes, polyploid evolution and crop domestication. *Nat. Genet.* 51, 865–876. doi: 10.1038/s41588-019-0402-2

Conflict of Interest: The authors declare that the research was conducted in the absence of any commercial or financial relationships that could be construed as a potential conflict of interest.

Publisher's Note: All claims expressed in this article are solely those of the authors and do not necessarily represent those of their affiliated organizations, or those of the publisher, the editors and the reviewers. Any product that may be evaluated in this article, or claim that may be made by its manufacturer, is not guaranteed or endorsed by the publisher.